UNCLASSIFIED

AD NUMBER	
AD014088	
CLASSIFICATION CHANGES	
TO:	**unclassified**
FROM:	**confidential**
LIMITATION CHANGES	
TO: **Approved for public release; distribution is unlimited.**	
FROM: **Distribution authorized to U.S. Gov't. agencies and their contractors; Administrative/Operational Use; JUN 1953. Other requests shall be referred to Army Materiel Command, Alexandria, VA.**	
AUTHORITY	
AMC ltr, 26 Mar 1981; AMC ltr, 28 Mar 1981	

THIS PAGE IS UNCLASSIFIED

UNCLASSIFIED

AD 14088

CLASSIFICATION CHANGED
TO: UNCLASSIFIED
FROM CONFIDENTIAL
AUTHORITY:
USAMC ltr
26 MAR 81

UNCLASSIFIED

COPY NO. 30

CONFIDENTIAL
SECURITY INFORMATION

INSTRUMENTATION FOR LOKI WIND MEASUREMENTS

by

Richard K. Smyth

Quarterly Report for Third Quarter
January 1, 1953 to March 31, 1953

June 1, 1953

Contract No. DA-04-495-Ord-352
Sub-RAD Order No. ORDTU 2-1106-7
Ordnance Project No. TU2-1012

CONFIDENTIAL
SECURITY INFORMATION

TABLE OF CONTENTS

ILLUSTRATIONS

ILLUSTRATIONS
(Continued)

PART 1

BALLOON-BORNE HOT WIRE ANEMOMETER SYSTEM

INTRODUCTION

In the development of the LOKI wind direction computer, statistical information on wind and gust distribution is required to establish appropriate wind sampling methods and to determine the values of the significant controlling parameters. The chief source of wind information for this purpose has been the data collected at the University of Michigan by Sherlock and Stout, Ref. 1. Vertical wind profiles extending up to 250 feet were obtained on a fixed tower during a number of winter storms in Michigan, using anemometers spaced at 25-foot intervals and capable of .1 second response. Preliminary analysis using small samples of the Michigan data indicates the possibility of calculating deflection corrections based on wind measurements with as few as one anemometer, Ref. 2. This work is continuing so that eventually some 5000 sequential wind profiles will have been analyzed. One shortcoming of the Michigan data is the limited altitude, burnout for LOKI occurring after 2,000 feet of trajectory. For a constant crosswind 50% of the deviation at burnout will be produced in the first 250 feet of trajectory, 66% during 400 feet, and 94% during 1,000 feet, Ref. 2.

Investigation to obtain space and time variations of wind within a volume of significant size has been set up under the sponsorship of the Signal Corps. This project

will involve the erection of several towers and the installation of a complex data recording system. Wind data will probably not be available before several months.

In view of the immediate need for wind information up to altitudes which could account for a significant portion of the deviation at burnout, the balloon-borne hot wire anemometer program was undertaken. In the initial phase a vertical arrangement of 5 anemometers is carried to a height of 1000 feet. If the initial work indicates the necessity for data to the full 2,000 feet, the height will be extended.

SYSTEM REQUIREMENTS

From the experience gathered in the study of the Michigan data, it was decided that a time resolution in the order of one second would be adequate for the wind record. Further it was felt that a minimum of 5 levels of observation would be required. A simplification in data reduction is effected if the levels are chosen at equal increments in the integrated wind effect. For the case of 5 levels the 20% increment will accumulate at 75, 175, 300, 600, and 2,000 feet. If the survey is terminated at 1,000 feet rather than 2,000 feet, an error of only a few percent is introduced. A recording system is required in view of the necessity for short-time resolution. A single channel direct writing recorder (Sanborn Model 141) shown in Fig. 1, capable of uniform response of the frequency range 0-50 cps, was available from another phase of the project and it was decided to utilize a data multiplexer system with this recorder in order to cover all channels with a sampling rate of one per second.

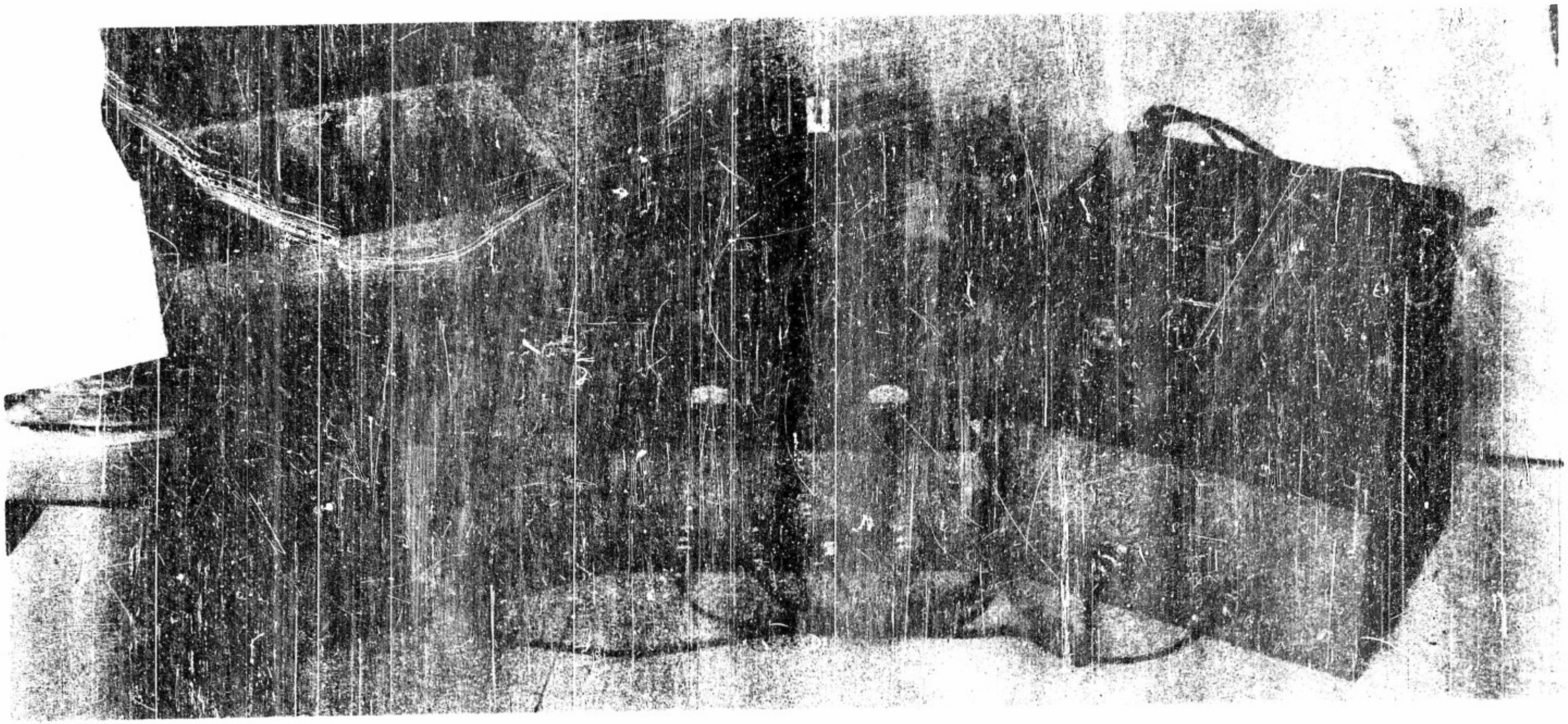

FIG. 1 — RECORDER AND CONTROLLER

It was considered desirable to make wind profile measurements in several locations including the Small Missiles Range at White Sands Proving Ground and for this reason the additional requirements of simplicity, portability, and mechanical ruggedness were added.

EQUIPMENT

The system chosen consists of a captive balloon supporting a cable which, in turn, carries a set of hot wire anemometers spaced at the intervals listed above, as shown schematically in Fig. 2. The hot wire anemometer is capable of the required response and can be made sufficiently light for the desired type of support. The balloon tethering line itself serves as the 6-conductor cable required for energizing and reading the hot wire. With this simple system direction can not be recorded and it is necessary for an observer to estimate direction from streamers attached to the line. Fig. 3 presents an operational block diagram for the overall system. The hot wire anemometer, five of which are shown in Fig. 4, consists of a one-foot length of temperature sensitive resistance wire strung in the form of an open grid across a 4-inch span. The support is a vane formed of light sheet aluminum and provided with two terminals for attachment to the tethering cable. The cable being weak in torsion allows the vane to keep the wire element headed into th wind. The total weight of the anemometer is about 2 ounces. To provide a sufficiently small time constant,

CONFIDENTIAL
SECURITY INFORMATION

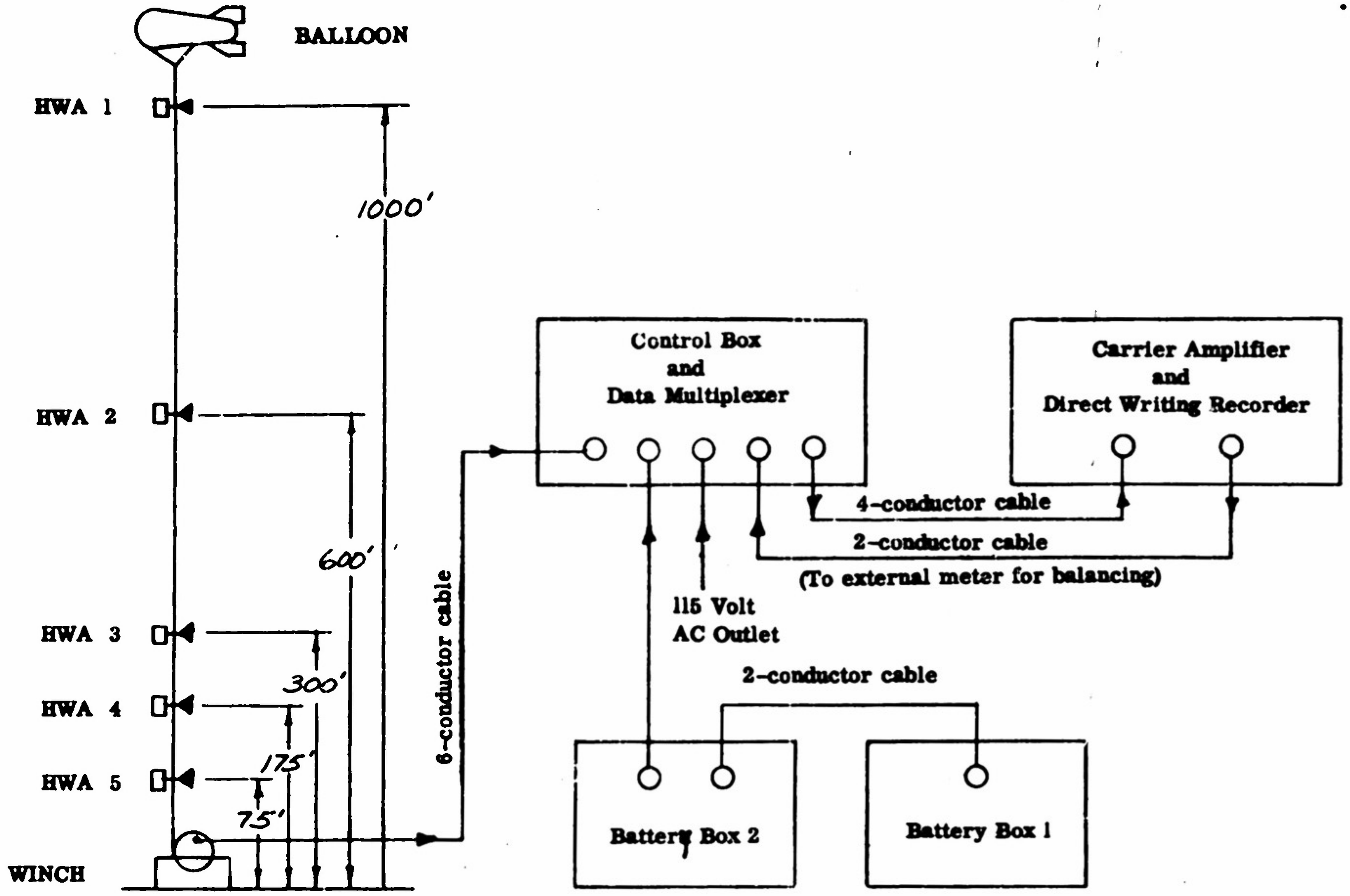

FIG. 2 SCHEMATIC BLOCK DIAGRAM

NORTH AMERICAN INSTRUMENTS INC.

CONFIDENTIAL
SECURITY INFORMATION

CONFIDENTIAL
SECURITY INFORMATION

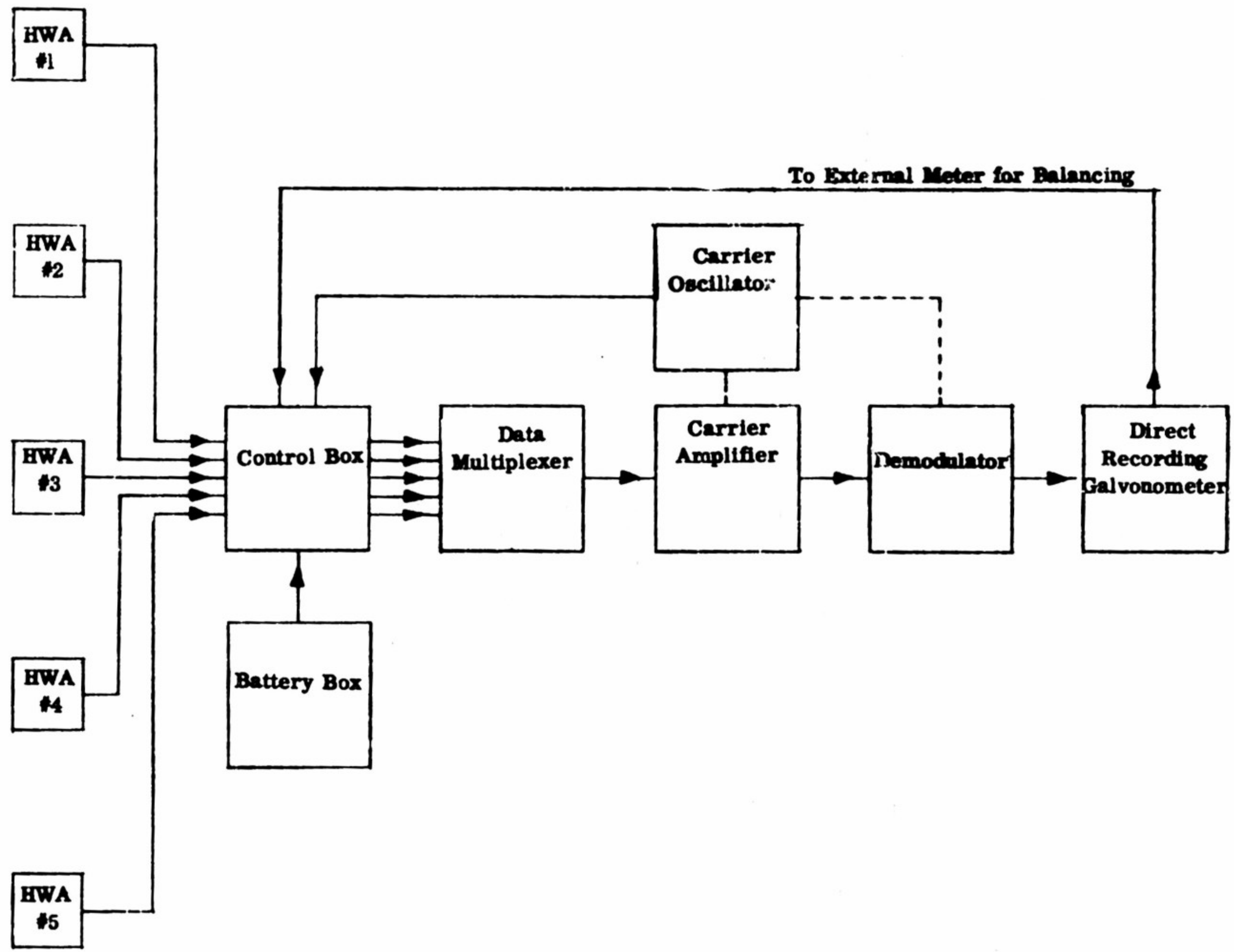

FIG. 3 OPERATIONAL BLOCK DIAGRAM FOR HOT WIRE ANEMOMETER INSTRUMENTATION

CONFIDENTIAL
SECURITY INFORMATION

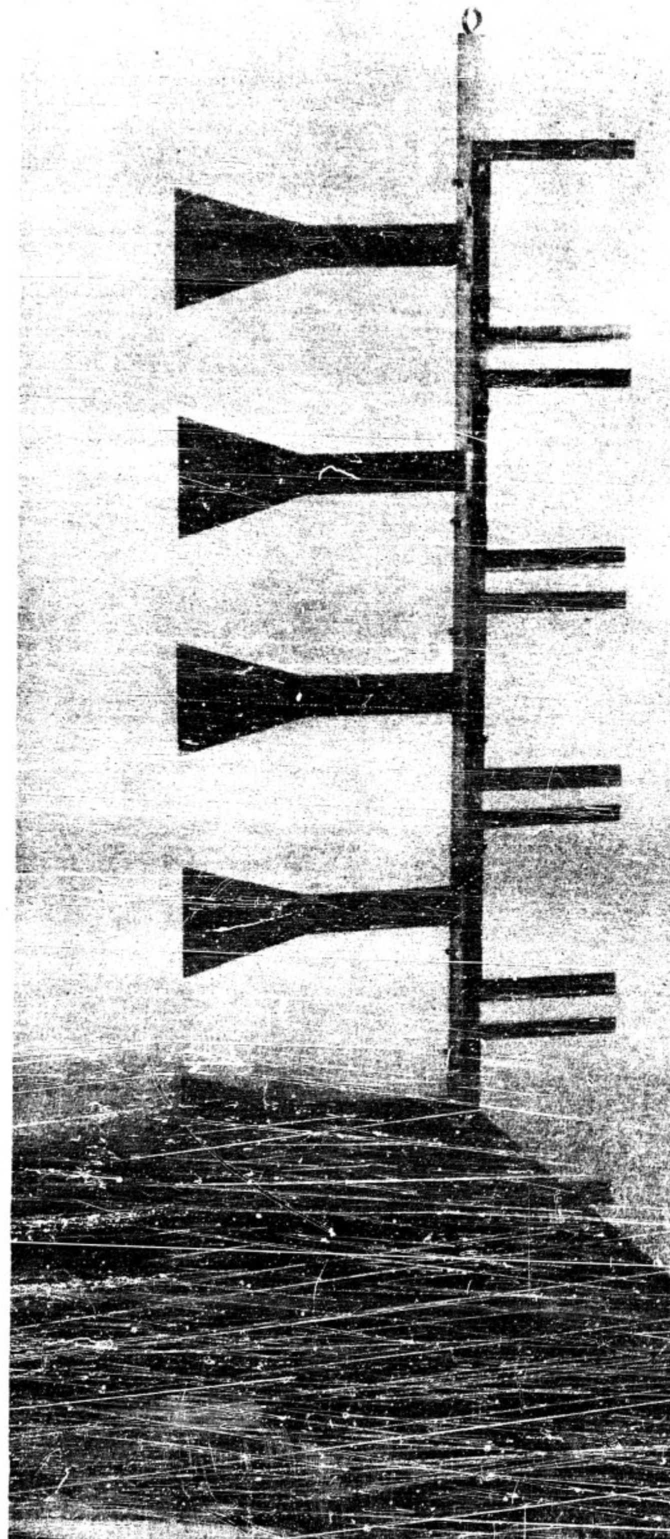

FIG. 4 - HOT WIRE ANEMOMETERS AND WIND TUNNEL FIXTURE

.001 inch diameter wire is used. The time constant of the anemometer was measured to be 0.2 second. The method for measuring the time constant is described in Appendix B. The material is Balco, a nickel-iron alloy with a linear temperature resistance characteristic, the temperature coefficient of resistivity being about 0.3% per degree F.

The hot wire anemometer element is heated by a constant d. c. current of about 65 m.a. which raises the wire temperature to about 350°F above ambient. The resistance of the wire which is a function of wind velocity, is measured in an a. c. bridge circuit.

The theory of the hot wire anemometer is described in Appendix A and circuit details are described in a separate section.

The balloon which supports the hot wire anemometers is of the non-rigid streamlined type and is manufactured by the Seyfang Laboratories. This balloon, shown in Fig. 5, has been used in similar investigations, Ref. 3 and Ref. 4. The static lift is 12 pounds. However, wind will provide an additional aerodynamic lift that can easily exceed this value by a considerable amount. The manufacturer advises against operation in winds exceeding 25 m.p.h. To comply with CAA Regulations and to facilitate recovery in the event of cable failure, an altitude actuated dump valve is provided to release the helium with which the balloon is filled at an altitude 1,000 feet

FIG. 5 - BALLOON AND WINCH AT EL MIRAGE AIRPORT

greater than the working altitude. A pressure relief system is incorporated in the design to limit the excess of internal pressure to 2 1/2 inches of water. The construction is shown in Fig. 6. The tethering line is a pair of vinyl covered 3-conductor cables reinforced with nylon string cord to provide a tensile strength of 100 pounds per cable. An electric motor driven winch, Fig. 7, is employed in reeling the balloon in and out.

The data multiplexer, which samples the 5 information channels for recording with the single channel Sanborn Recorder, is built around a relay operated stepping switch (Automatic Electric Company Model 45). The stepping switch has 10 banks of contacts in 26 positions. The first four banks carry the anemometer signals and the fifth is connected to a set of pilot lights to indicate the active channel. The circuits are connected with channel 1 occupying the first two positions, the other 4 channels following in sequence. Thus, one complete cycle requires 6 positions. The sampling cycle is repeated 4 times for each complete cycle of the stepping switch. The remaining 2 positions of the 26 available are left open, providing a reference mark for data reduction. During automatic operation, the switch is stepped by a motor driven cam-microswitch arrangement, providing a 1.2-second 5-channel scanning cycle. A push button is provided for manual stepping during checkout.

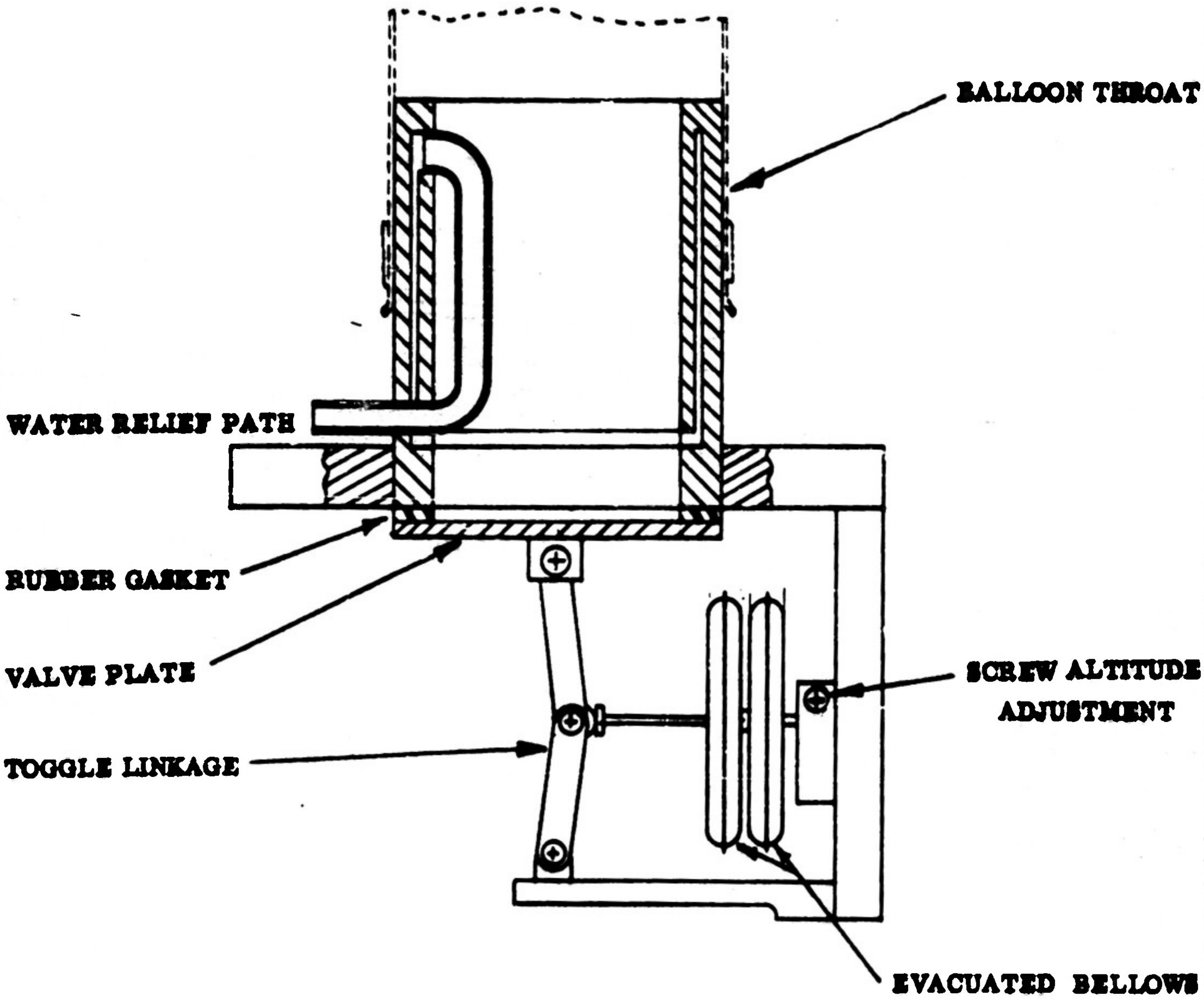

FIG. 6 BALLOON DUMP VALVE SCHEMATIC

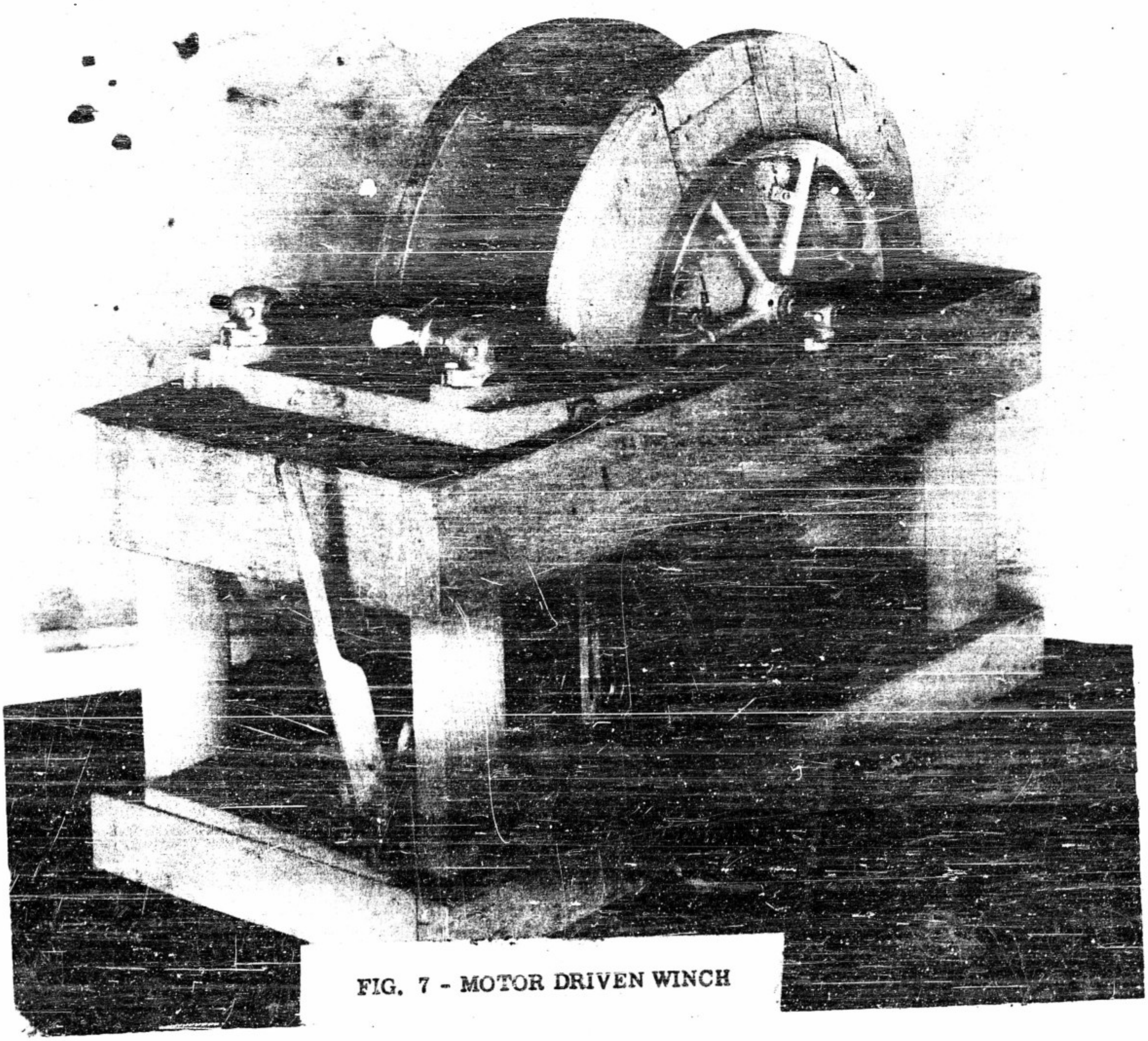

FIG. 7 - MOTOR DRIVEN WINCH

All circuits are completed in a central control box, which also houses the stepping switch. Controls are provided for excitation, balance, and circuit standardization for change over from wind to temperature measurement.

Batteries are used for the d. c. hot wire excitation. These are housed in 2 boxes, 12 45-volt batteries in each.

CIRCUITRY

The circuit may be divided into two operationally separate parts, one d. c. for heating, and the other a. c. for measuring. These are treated separately below in detail.

The d. c. circuit, Fig. 8, consists of the series arrangement of the battery bank, the adjustable dropping resistor, the m. a. meter, and the five hot wire elements shunted by the other three arms of the wheatstone bridge. The meter measures the current drain from the batteries. This current is divided between the hot wire element and the other three arms of the wheatstone bridge, with approximately 65% of the meter current passing through the hot wire elements.

The carrier frequency circuit, Fig. 9, is a wheatstone bridge. One arm is the hot wire element and a series equalizing resistor; the adjacent arm has an equal resistance, a small part of which is a potentiometer for resistive balance control.

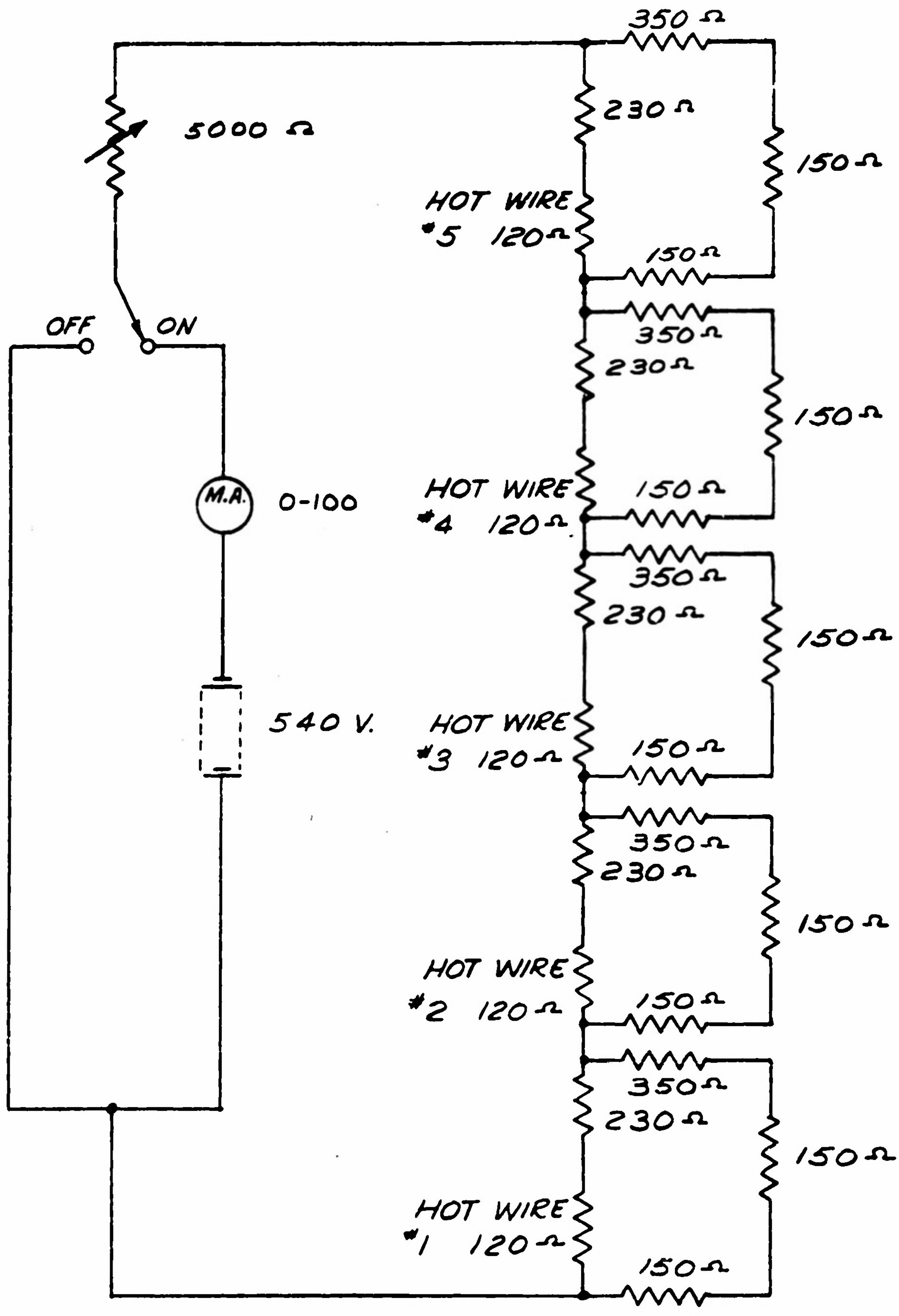

FIG. 8 DC CIRCUIT SCHEMATIC

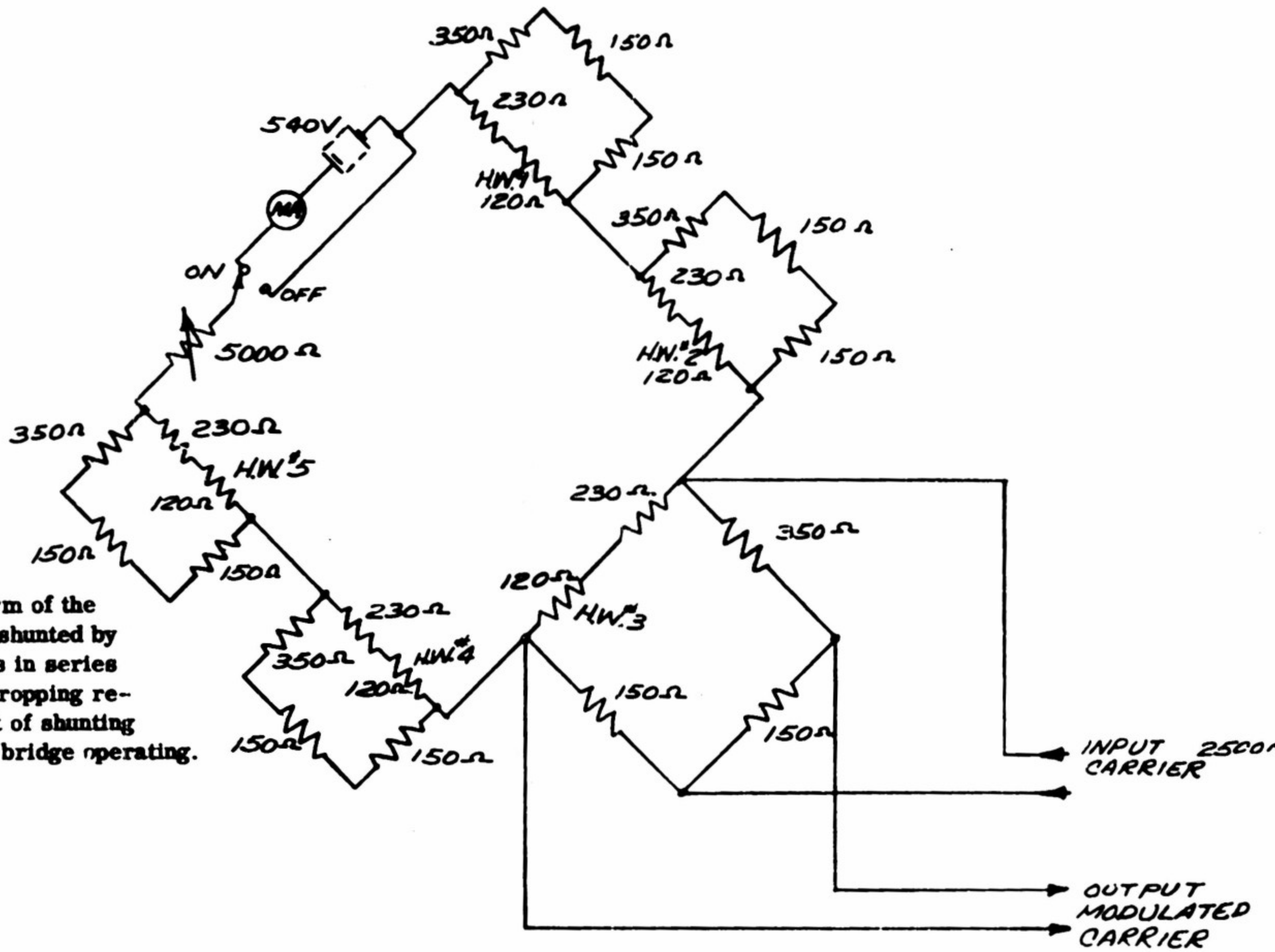

Note: The active arm of the operating bridge is shunted by all the other bridges in series with the 5000 ohm dropping resistor. The amount of shunting is the same for any bridge operating.

FIG. 9 CARRIER FREQUENCY CIRCUIT SCHEMATIC SHOWING CHANNEL 3 OPERATING

The other two arms are precision 150 ohm resistors. The reactive balance is provided by shunting the input with a 25K ohm potentiometer, the center tap being connected to the grounded corner of the bridge through a 0.2 μf capacitor. Three 2 μf capacitors are employed to block the d.c. from the input transformer windings of the carrier amplifier.

The changes in resistance of the heated wire element due to wind cooling provide the carrier modulation. This modulated wave is amplified, demodulated and rectified, with the resulting d.c. signal being applied to the galvanometer element of the recorder. The constant d.c. heating current has no effect on the carrier frequency circuit.

The circuit for temperature measurement is the same as that for wind measurement with the exception that the d.c., excitation is removed. The a.c. carrier current is not sufficient to cause an appreciable temperature rise in the wire, so that essentially ambient temperature effect is measured. For circuit standardization in the field, a known wind or temperature may be simulated by shunting a precision resistor across one arm of the bridge.

CALIBRATION

The anemometers were calibrated in the Merrill Wind Tunnel at the California Institute of Technology. The tunnel has a vertical span of 36 inches with a velocity distribution constant within 1% over the space used. Velocity runs from 6.4 mph to 50 mph

were made with 5 anemometers at a time, using the fixture shown in Fig. 4. Three runs were made interchanging anemometers, in order to determine if the anemometers would all have the same characteristics. Each channel was balanced with zero heater current. The calibration procedure consisted of recording the zeroes for each channel. A calibration signal was applied for each channel and recorded. The wind signal was then recorded for each channel. This procedure was followed for each velocity setting.

The deflection from the zero level to the wind level is measured for a given channel. The deflection from the zero level to the calibration signal is then measured. The calibration curve is the ratio of wind deflection to calibration deflection plotted as a function of wind velocity for each channel. A typical calibration curve is shown in Fig. 10.

The calibration results indicate that all the anemometers have approximately the same characteristics. Fig. 11 is a plot of output versus wind velocity for three different anemometers placed in the same channel.

CONFIDENTIAL
SECURITY INFORMATION

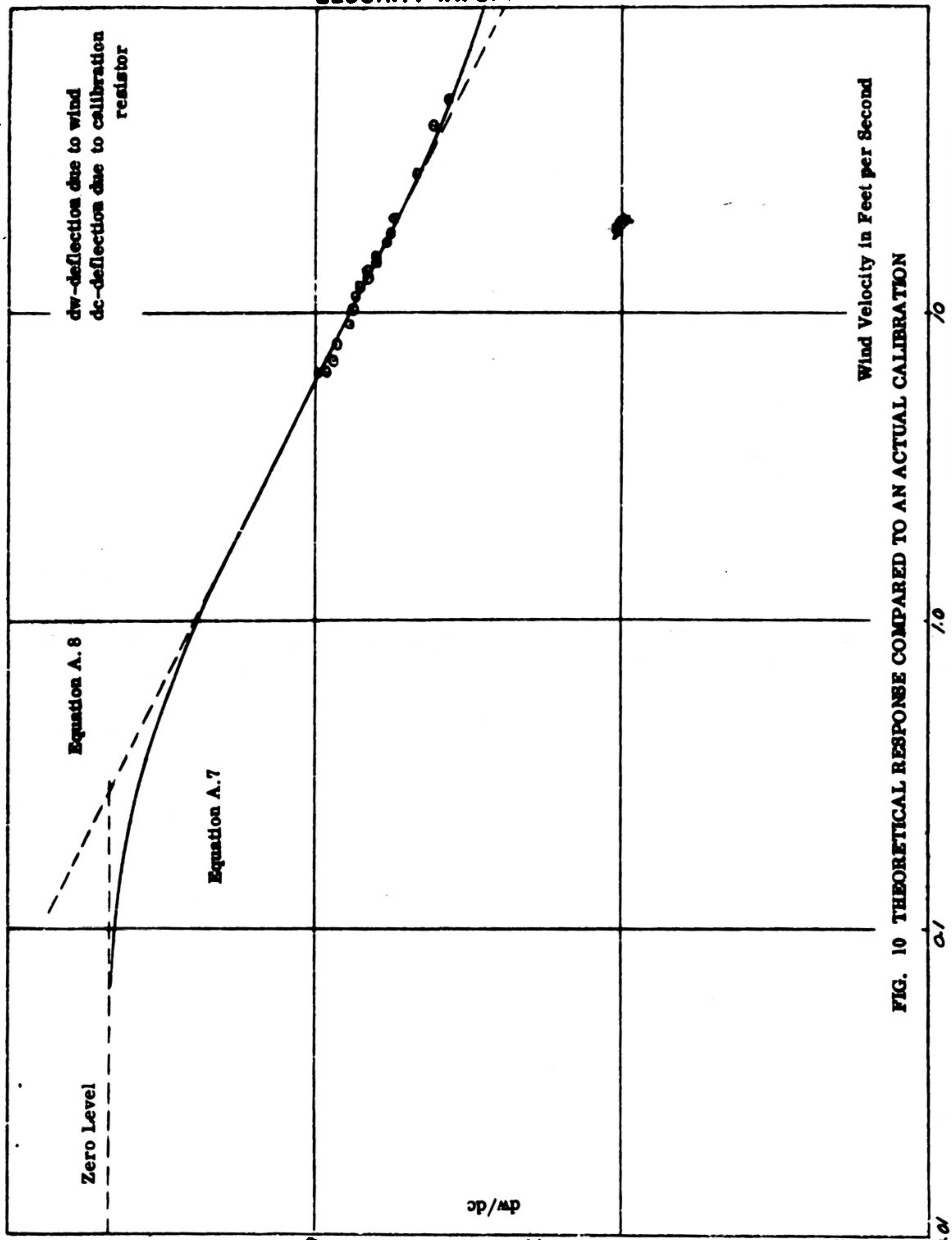

FIG. 10 THEORETICAL RESPONSE COMPARED TO AN ACTUAL CALIBRATION

NORTH AMERICAN INSTRUMENTS INC.

CONFIDENTIAL
SECURITY INFORMATION

HOT WIRE ANEMOMETER

CALIBRATION CURVE

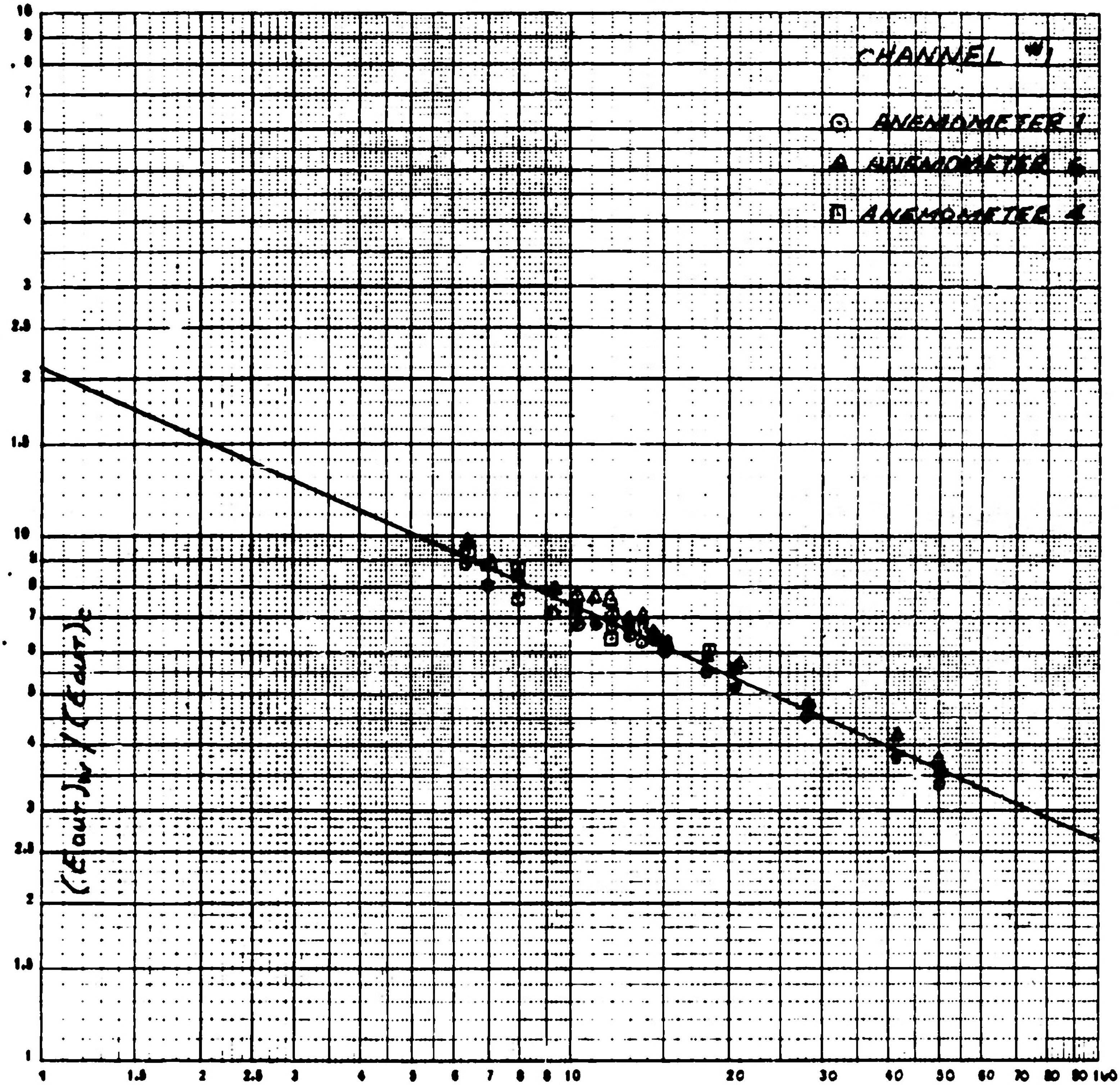

FIG 11

FIELD OPERATIONAL PROCEDURE

Balloon Handling

The balloon is filled with helium, 2 1/2 cylinders being required, and sand-bagged in place. The fins are attached and the dump valve set and inserted in the throat. The balloon is then "walked" to the motor-driven winch and the bridle is attached to the tethering cable.

The cable is reeled out and anemometers attached as the plugs appear. Colored streamers are attached at 50-foot intervals for aircraft warning. Reverse procedure is followed in bringing down the balloon. For overnight storage the balloon may be sand-bagged in a sheltered location with the tail fins removed.

Electrical System Balancing

Each element is balanced for temperature operation as it is attached into the cable circuit. The ambient temperature is read from a separate thermometer to establish the calibration level. After all elements are air-borne they are balanced for operation as anemometers with zero heating current, as in the calibration procedure.

Recording

The zero levels for each channel are set at one side of the tape and the heater current is adjusted to the operating level. The gain is adjusted so that the maximum anticipated wind range corresponds to full scale deflection. The system is standardized

by recording zero and velocity calibration signals at zero heater current. The heater current is applied and monitored at 100 milliamps while the wind run is taken.

APPENDIX A

THEORETICAL ANALYSIS OF THE HOT WIRE ANEMOMETER

King's Equation

The basic equation for the thermal equilibrium of an electrically heated wire immersed in a flowing fluid, originally derived by King, Ref. 5, is:

$$i^2 R = (a + bV^{1/2}) \quad \frac{R - R_a}{\alpha R_o} \qquad \text{Equation A. 1}$$

where:

i = current passing through the wire in amps
R = resistance of the wire with the current passing
R_a = resistance of the wire at the ambient air temperature
α = temperature coefficient of resistance
$\underline{a}$ and $\underline{b}$ are constants dependent upon the geometry and physical characteristics of the wire (these are most easily determined empirically)

Solving equation A. 1 for $\underline{R}$ we obtain

$$R = R_a \left[\frac{(a + bV^{1/2})}{(a + bV^{1/2} - \alpha R_o i^2)} \right] \qquad \text{Equation A. 2}$$

Since we are interested in the resistance change from the "cold" resistance $\underline{R_a}$ in our bridge circuit operation, the expression for $\Delta R = R_a - R$ is given below

$$\Delta R = R_a \left[1 - \frac{(a + bV^{1/2})}{(a + bV^{1/2} - \alpha R_o i^2)} \right] \qquad \text{Equation A. 3}$$

Hot Wire Anemometer Sensitivity

It may be shown from equation A. 1 that the sensitivity of the hot wire anemometer decreases as the wind velocity increases. Taking the partial derivative of R with respect to V at constant current, we obtain from Equation A. 1

$$\left(\frac{\partial R}{\partial V}\right)_{i=\text{const}} = - \frac{R(R - R_a)}{2R_a\left(V + \frac{a}{b} V^{1/2}\right)} \qquad \text{Equation A. 4}$$

We may define $\left(\partial R/\partial V\right)_{i=\text{const}}$ as the wind sensitivity of the hot wire anemometer. It is apparent from Equation A. 4 that

a) $\lim\limits_{V \to 0} \left(\frac{\partial R}{\partial V}\right)_i = \infty$

b) $\lim\limits_{V \to \infty} \left(\frac{\partial R}{\partial V}\right)_i = 0$

These two results illustrate that in the region of very low velocity the hot wire anemometer output is extremely sensitive to changes in velocity. At high velocities the hot wire anemometer output is relatively insensitive to velocity changes.

<u>Hot Wire Connected in Wheatstone Bridge</u>

The output of the hot wire bridge used (Fig. 9) is derived in this section. The bridge is initially balanced with zero heater current. This means that $R = R_a$ during balance. The bridge output in terms of any resistance change $\Delta R = R_a - R$ is given by

$$E_{out} = E_{in} \frac{150 \Delta R}{(350 + 150)\ (350 + 150 + \Delta R)} \qquad \text{Equation A. 5}$$

Assuming $\Delta R << 500$ then we obtain from equation A. 5

$$E_{out} = 0.0006\ E_{in}\ \Delta R \qquad \text{Equation A. 6}$$

Substituting the expression equation A. 3 for ΔR into equation A. 6 we obtain

$$E_{out} = 0.0006\ E_{in}\ R_a \left[1 - \frac{(a + bV^{1/2})}{(a + bV^{1/2} - \alpha R_0 i^2)} \right] \qquad \text{Equation A. 7}$$

We may check equation A. 7 by investigating the bridge output at the extreme conditions:

1) If $i = 0$, then $E_{out} = 0$, independent of the wind velocity
2) If $i = 0.100$ amp and $V = 0$, then $E_{out} = 0.0006\ E_{in}\ R_a$
3) If $i = 0.100$ amp and $V \rightarrow \infty$, then $E_{out} \rightarrow 0$

These three results agree qualitatively with the observed output of the bridge at the extreme conditions.

In the range of calibration 9-75 ft/sec a plot of bridge output versus wind velocity was found to agree with a simplified form of equation A. 7.

$$E_{out} \approx -0.0006\ E_{in}\ R_a \frac{a}{b\ V^{1/2}} \qquad \text{Equation A. 8}$$

Equation (A. 8) may be derived from equation (A. 7), if the following assumptions are made:

(1) $a \gg bV^{1/2}$

(2) $bV^{1/2} \gg (a-\alpha R_o i^2)$

In Fig 10 the two theoretical response curves corresponding to equations A. 7 and A. 8 are fitted to the experimental calibration points. It is apparent that equation A. 8 will apply for velocities as low as 1 ft/sec within the limits of observational accuracy.

APPENDIX B

EXPERIMENTAL METHOD FOR DETERMINING THE TIME CONSTANT OF THE HOT WIRE ANEMOMETER

The nature of the circuit used with the hot wire anemometer installation allows a very simple method for determining the time constant. The bridge is energized at carrier frequency and the hot wire element is heated by a separate d. c. source. If the heater current is switched on or off, then the effect on the bridge output will be identical to that of a step function wind. The time constant may then be determined directly from the resulting bridge output trace. It is assumed that the electrical time constant is negligible compared to the hot wire anemometer time constant. This assumption appears reasonable, since the d. c. circuit is almost purely resistive.

It may be shown, Ref. 6, that the hot wire anemometer time constant is a function of wind velocity. The equation is

$$M = \frac{4.2\ m\ s}{R_0\ \alpha\ (A + B\ V^{1/2})} \qquad \text{Equation B.1}$$

where
- M = time constant in seconds
- m = mass of wire
- s = specific heat of wire material
- R_0 = resistance of wire at zero degrees centigrade
- α = coefficient of resistivity of wire
- V = wind velocity
- A, B are constants

Note from equation B. 1 that the maximum time constant occurs at $V = O$ for which case $\underline{M}$ becomes

$$M_0 = \frac{4.2 \, m \, s}{R_0 \, \alpha \, A} \qquad \text{Equation B. 2}$$

Fig. 12 shows a typical record obtained by applying the step function "wind". This record was taken at zero wind and therefore represents the maximum time constant $\underline{M_0}$. The observed value of $\underline{M_0}$ is approximately 0.2 seconds.

FIG. 12 HOT WIRE ANEMOMETER STEP FUNCTION RESPONSE

APPENDIX C

DISCUSSION OF ERRORS

Intermodulation Errors

Since the five hot wire anemometer bridges are interconnected, the output of a given bridge will be affected by variations in the other four bridges. Consider Fig. 9, which shows the carrier frequency circuit. The active arm of the bridge is shunted by the other four bridges in series with the dropping resistor. If the wind is constant for a given bridge and the wind on the other four bridges is varied from zero to infinity, the change in the effective resistance of the active arm of the given bridge is about 1/2 ohm. This extreme condition represents a maximum intermodulation error of about 1%.

Heater Current Fluctuations

If it is assumed that each hot wire changes 50 ohms in resistance (the maximum possible change), we may calculate from the circuit of Fig. 8 that the change in heater current will be approximately 6%. From the results of Appendix A, we note that the bridge output is virtually insensitive to heater current changes over the useful velocity range. The error from changes in heater current may therefore be considered negligible.

Ambient Temperature Changes

Temperature changes will affect the zero load and the wind output level because of the change in R_a (see Appendix A). The temperature fluctuation during a typical run is small and the temperature error would not be more than 2% maximum.

Calibration Error

The wind tunnel calibration is good to within 1% at the high velocities (15-50 mph) and within 10% at the low velocities (6-15 mph). The smoothing of the experimental points, however, should give an estimated error of 2%. Another source of error in calibration arises from the assumption that all the anemometers have the same characteristics. The error introduced from this assumption would increase the overall calibration error to approximately 3%.

Overall System Error

Taking into account all the possible sources of error it is believed that the overall system error is less than 5% of the reading over the range of velocities of 5-50 ft/sec, and 10% of the reading over the range 0.5-5 ft/sec.

PART 2

TWO-COMPONENT ANEMOMETER PROTOTYPE WIND TUNNEL TESTS

A survey of existing instrumentation made at the beginning of the LOKI Wind Correction Computer Project indicated the advisability of developing an anemometer particularly suited to the computer application. A design was chosen that would allow a time constant of as little as one second and also provide orthogonal wind components.

A brief description of the prototype model is contained in Ref. 7. The instrument consists of a vertical cylindrical column 3 inches in diameter and 18 inches long, incorporating two sensing elements as shown in Fog. 13. Each cylindrical sensing element is supported internally to measure the component of wind force along one axis and the elements are stacked with their sensitive axes mutually perpendicular to provide orthogonal components of the wind force. The construction is shown in the section drawing, Fig. 14, and in photograph, Fig. 14a. The supporting leaf springs deflect in proportion to the wind load and the deflection is measured and transmitted by a differential transformer. The mechanism is counterbalanced to eliminate mechanical vibration and position errors.

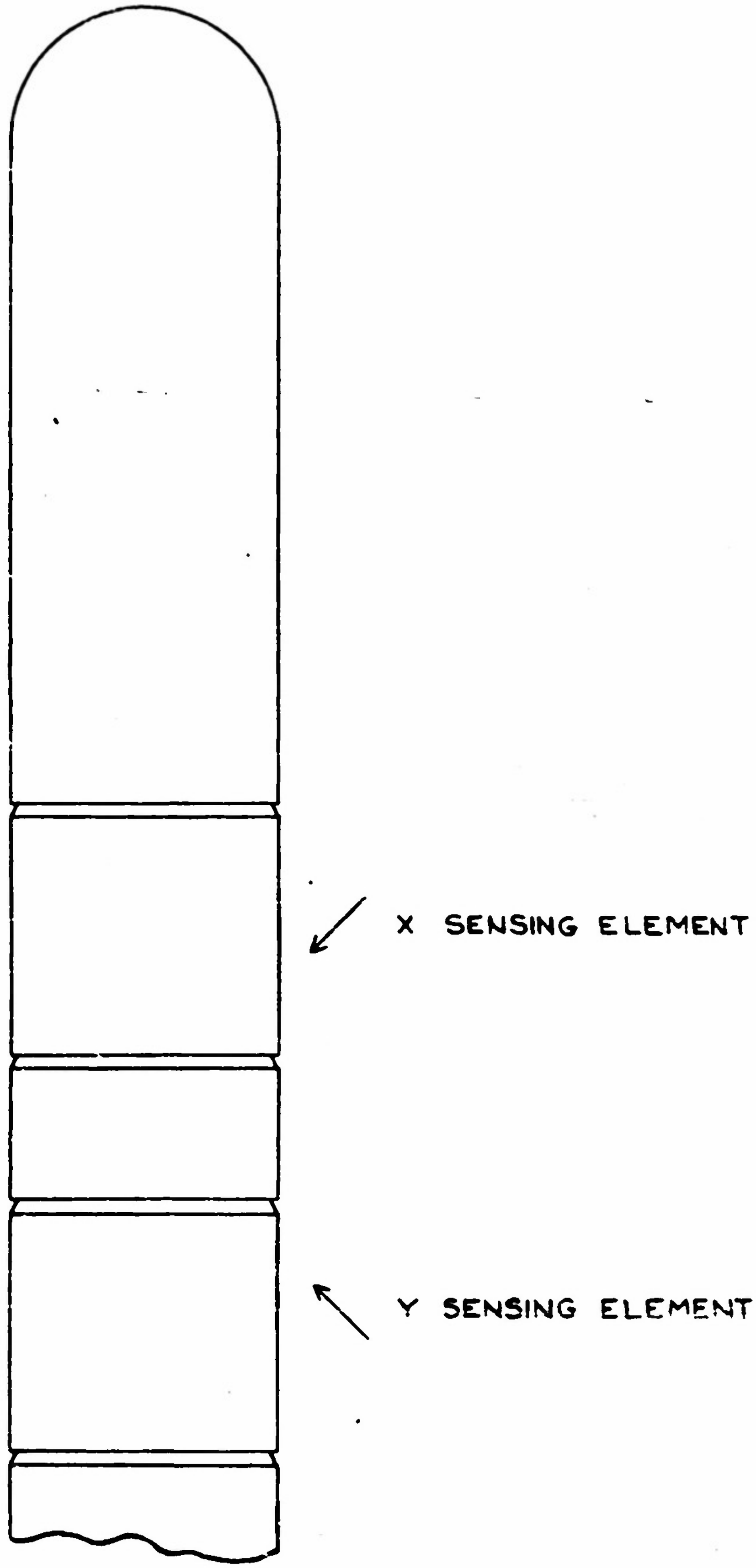

FIGURE 13
ANEMOMETER OUTLINE (1/2 SIZE)

NORTH AMERICAN INSTRUMENTS, INC. Oct. 1952

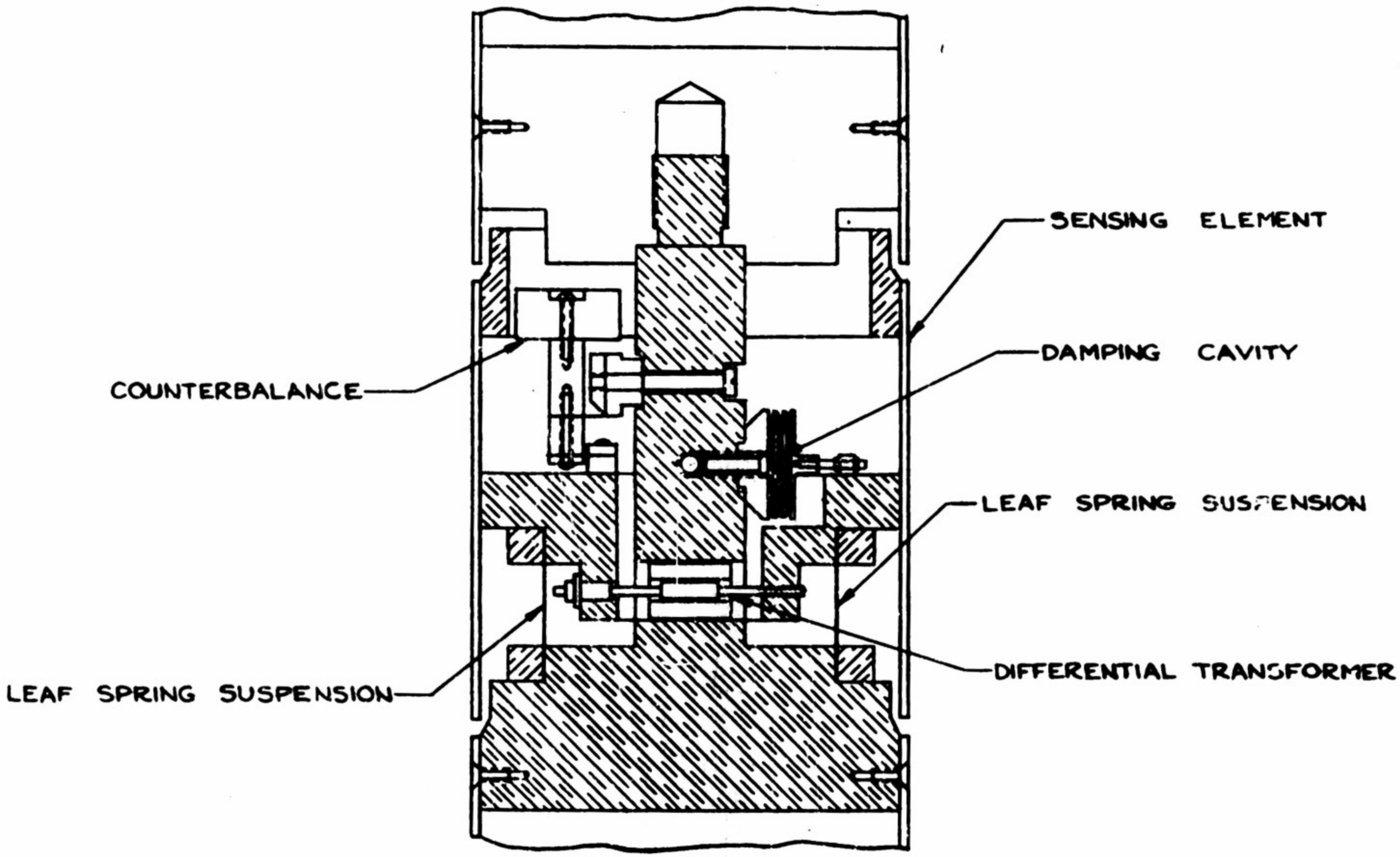

FIGURE 14
ANEMOMETER CROSS-SECTION

NORTH AMERICAN INSTRUMENTS, INC. Oct. 1952

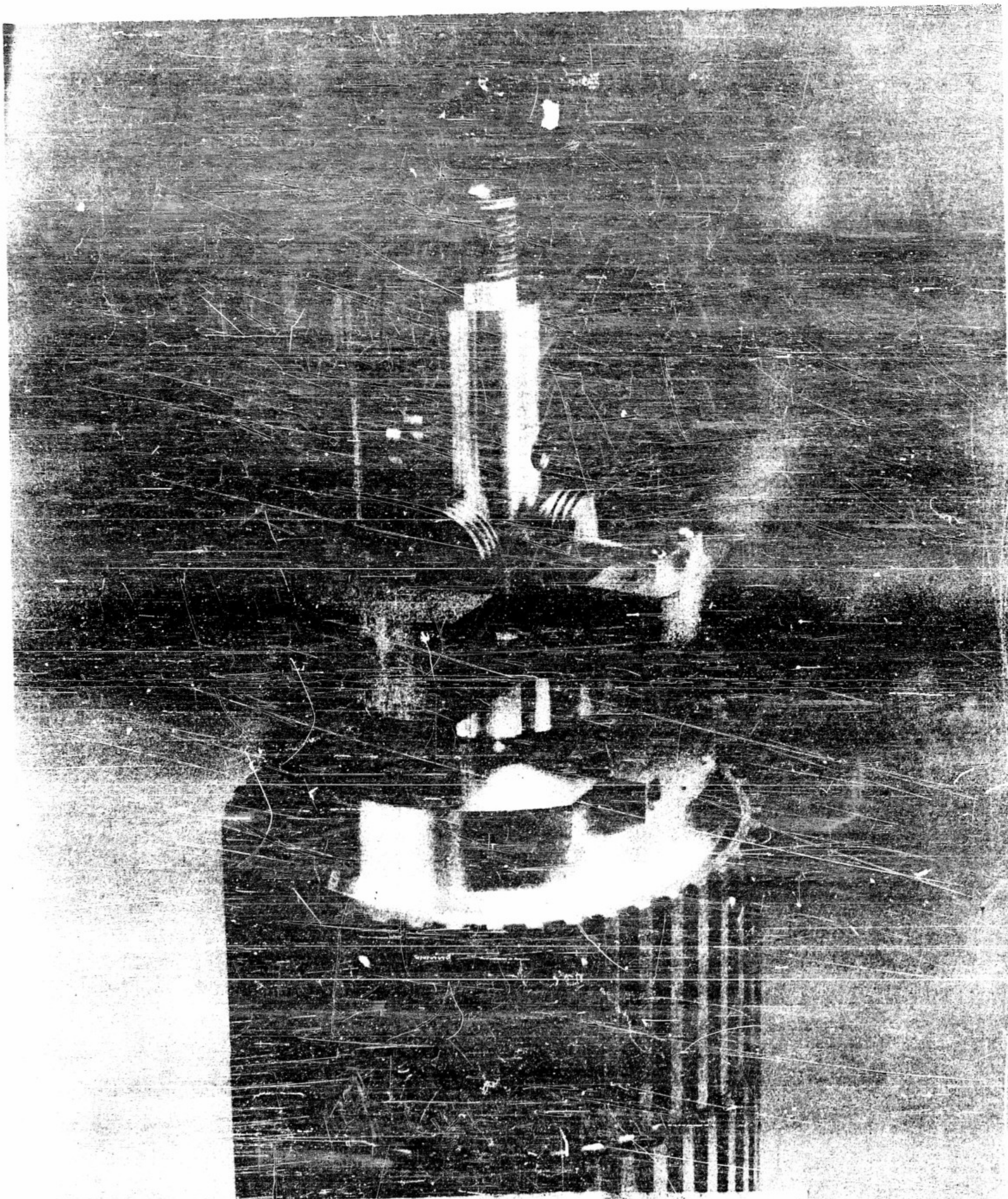

FIG. 14a TWO COMPONENT ANEMOMETER ELEMENT

Calibration tests of the original prototype at the Merril Wind Tunnel at the California Institute of Technology up to wind velocities of 70 m.p.h. (Reynolds No. 1.6×10^5) indicated satisfactory performance in regard to force resolution and constancy of drag coefficient at low speeds. However, fluctuating lift forces as great as 60% of the drag were observed at the higher speeds. The effect was traced to surface condition and most of the subsequent development has been directed toward the elimination of the lift through roughening of the surface. A satisfactory surface roughening consisting of vertical milled slots has been arrived at. This configuration provides stability within 2 mph up to wind speeds of 70 mph. Additional improvements in the method of counterbalance suspension, and in dust sealing have been made and a second prototype model is being built for field testing.

CALIBRATION TESTS FOR THE ANEMOMETER SERIES

All calibrations were made in the Merrill Wind Tunnel at the California Institute of Technology in a wind velocity range of 0-70 mph (Reynolds No. $0-1.6 \times 10^5$). The recording system is shown in the block diagram, Fig. 15, and is built around a Sanborn Model 141 Carrier Amplifier Recorder fed by a differential transmitter in the anemometer element. Plots of recorder trace amplitude against wind pressure, a quantity proportional to the square of the velocity, are made for the various configurations along with polar plots of trace amplitude vs. angle between wind

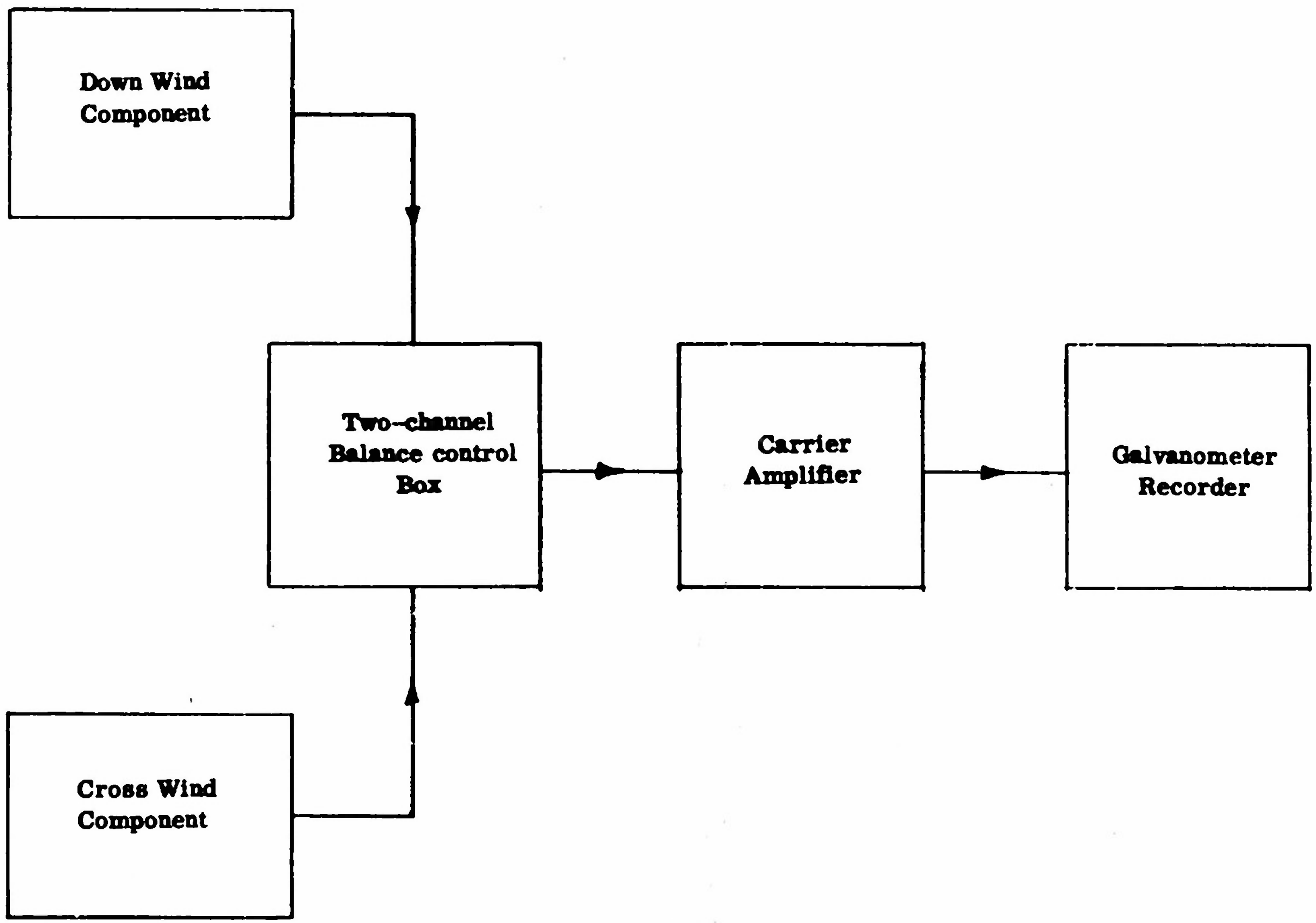

FIG. 15 TWO COMPONENT ANEMOMETER RECORDING SYSTEM BLOCK DIAGRAM

NORTH AMERICAN INSTRUMENTS INC.

direction and the sensitive axis for constant wind velocity. For true square law response (constant drag coefficient) the former plot should be linear and for cosine resolution the polar plot should be circular.

The calibration curve for the prototype model with smooth surface is shown in Fig. 16. The deviation from the best straight line through the observed points is less than 2 mph. The polar plots, Fig. 17, indicate satisfactory resolution at wind speeds below 70 mph. At this upper limit a lobe occurs at about 78°.

During the calibration an instability phenomenon was observed, not shown in the curves. With the sensitive axis of the anemometer perpendicular to the tunnel axis, a fluctuation in output was observed at velocities above 20 mph. The time interval between output shifts was in the order of a few seconds. A sample record is shown in Fig. 18. At a velocity of 60 mph the fluctuation corresponds to a peak lift force of about 60% of the drag force. The relative effect decreases at lower velocities; at 30 mph the lift force is approximately 5% of the drag.

Since the anemometer is to be used in measuring components, the fluctuating lift effect cannot be tolerated. From the nature of the phenomenon it was felt that the triggering mechanism might be a transition from laminar to turbulent flow with the resultant assymetrical shifting in flow separation on either side. The literature, Ref. 8, indicated that the effect might be minimized by roughening the surface.

CONFIDENTIAL
SECURITY INFORMATION

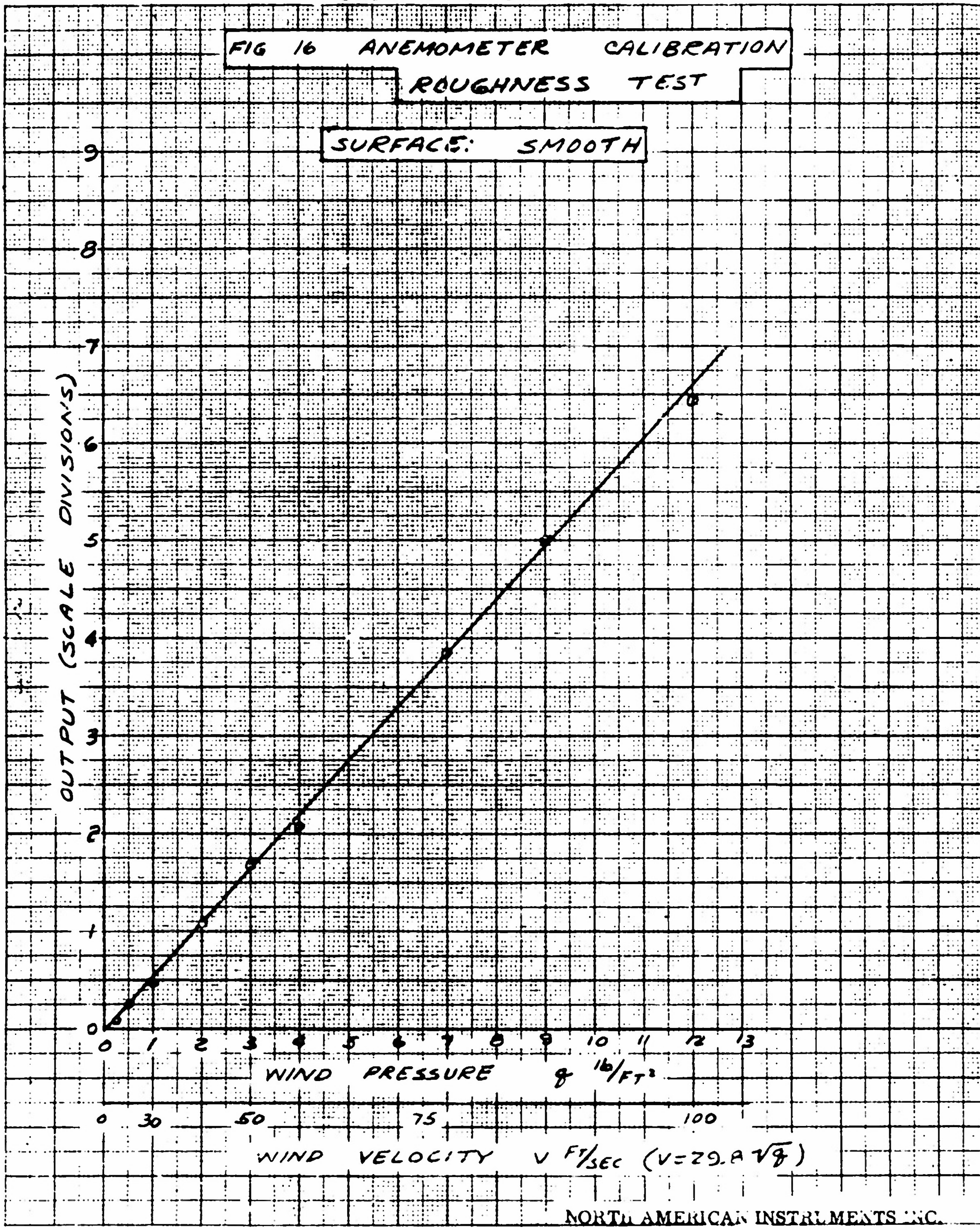

CONFIDENTIAL
SECURITY INFORMATION

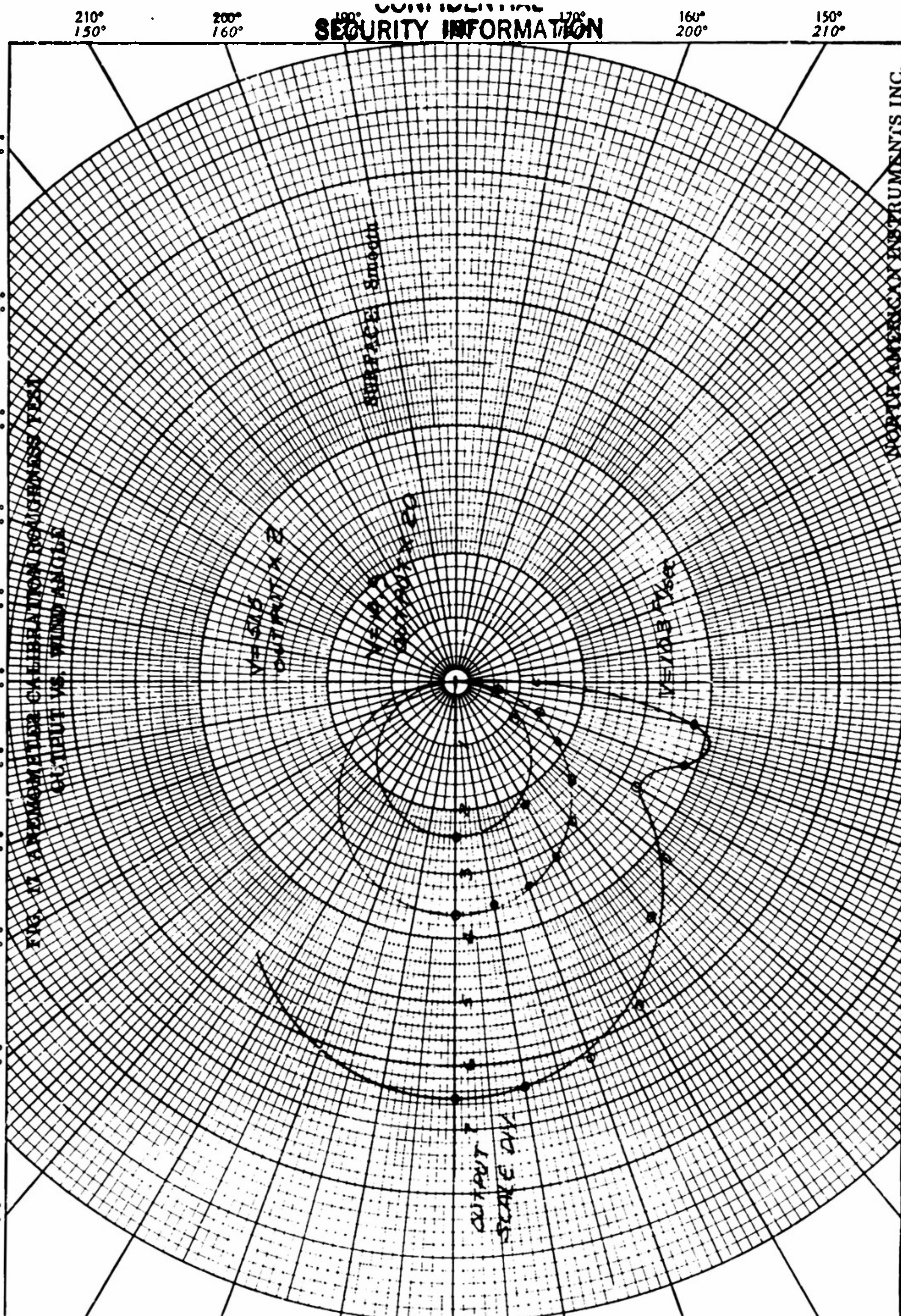

FIG. 17 ANEMOMETER CALIBRATION ROUGHNESS TEST OUTPUT VS. WIND ANGLE

SURFACE: Slots 1/16" Deep x 1/16" Wide x 1/18" Spacing

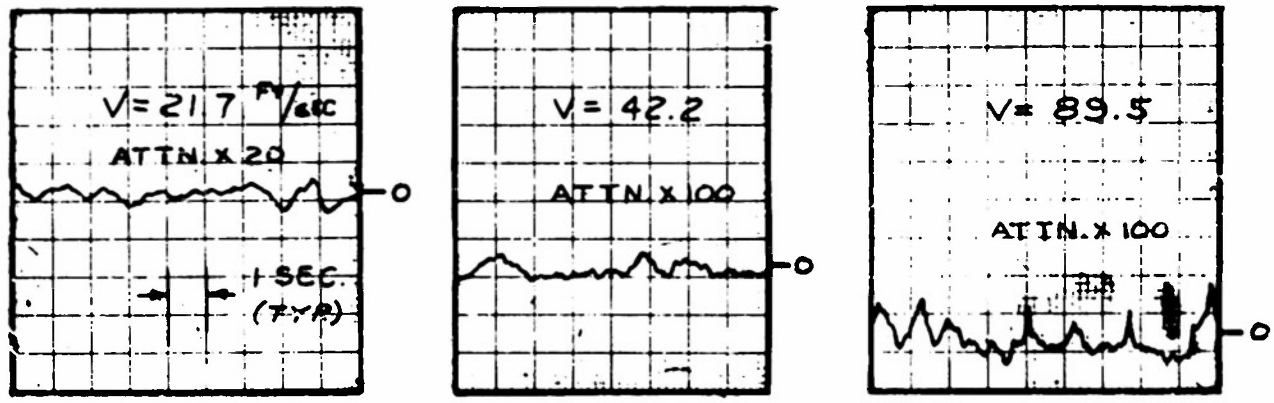

SURFACE: Knurled + 1/4" Mesh Wire

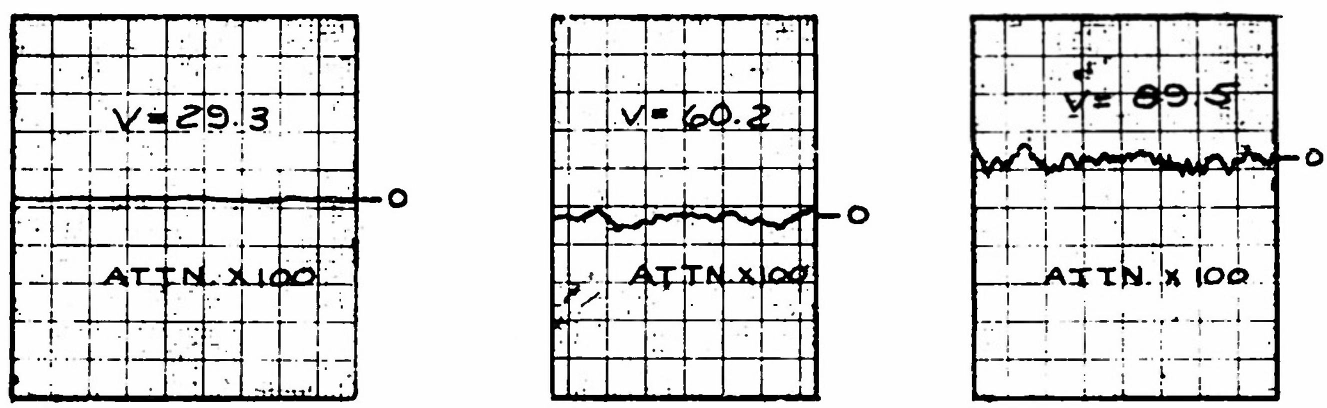

SURFACE: Slots 1/16" Deep x 1/8" Wide x 1/8" Spacing

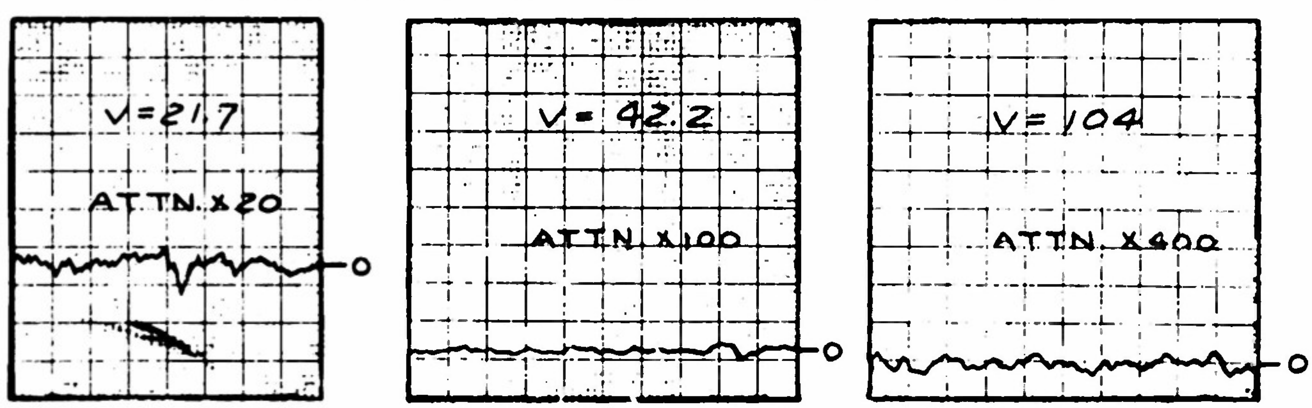

FIG. 18 ANEMOMETER RESPONSE RECORDS FOR CONSTANT CROSSWIND
Page 1 of 2

SURFACE: Smooth

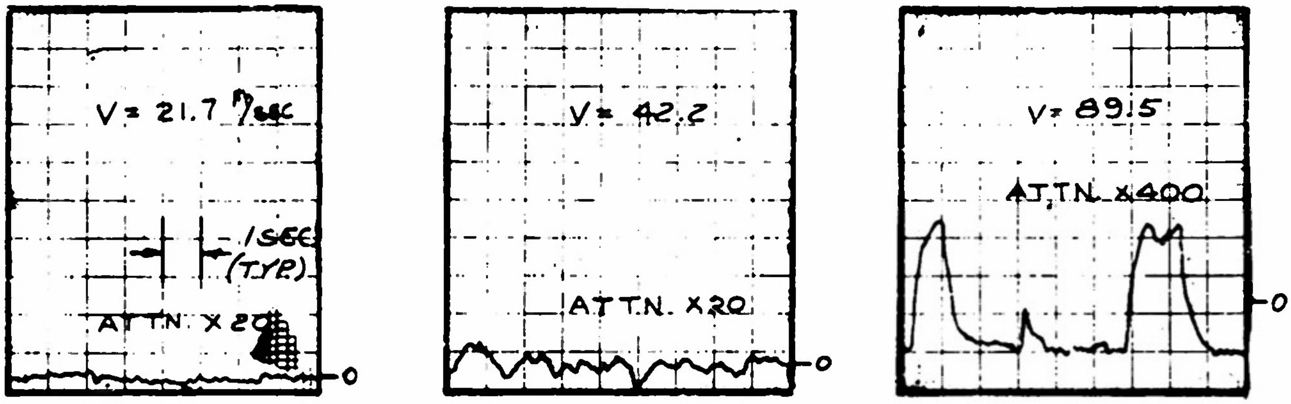

SURFACE: Knurled

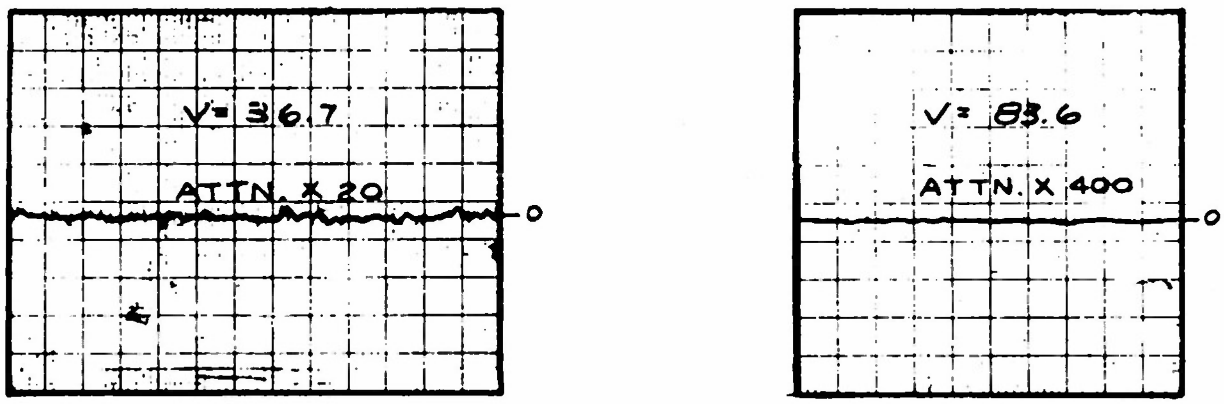

SURFACE: Knurled

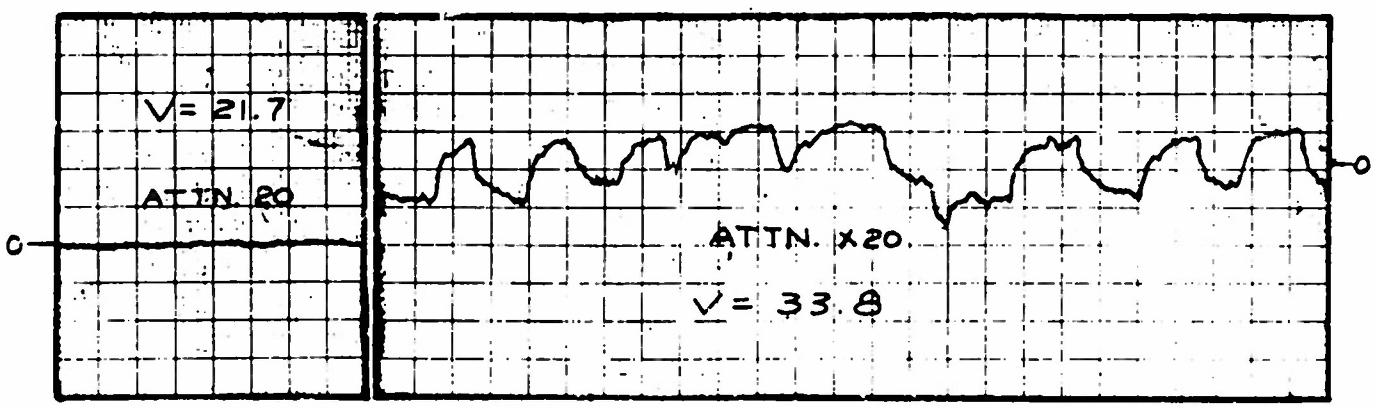

FIG. 18 ANEMOMETER RESPONSE RECORDS FOR CONSTANT CROSSWIND
Page 2 of 2

A number of configurations were tried in studying the effect of surface roughness. These included deep knurling, vertical transition wires cemented to the surface, 1/4 inch wire mesh taped to the surface, and vertically fluted sleeves attached over the anemometer elements.

The calibration curves corresponding to deep surface knurling are shown in Figs. 19 and 20. An abrupt change in slope of the pressure vs. output plot occurs at about 33 mph ($R = 7.5 \times 10^4$) corresponding to an increase in drag coefficient with velocity. The fluctuating lift effect was present with a peak at about 20 mph of about 26% of the drag force. The polar plot indicates a serious departure from the cosine law.

In view of the poor results shown in the knurling tests, it was decided to investigate the effect of gross roughness. For the initial test vertical wires were cemented to the surface of the sensing cylinder at various angular locations to induce flow separation. Observations are shown in Fig. 21.

To test the effect of complete surface roughness with elements the size of the transition wires, sleeves were made of wire screen with an open square quarter-inch mesh. The wire diameter was 1/64 inch. With these sleeves attached over the anemometer elements, the calibration curve, Fig. 22, was obtained. The output-V^2 plot fits a straight line and the maximum departure of observed points

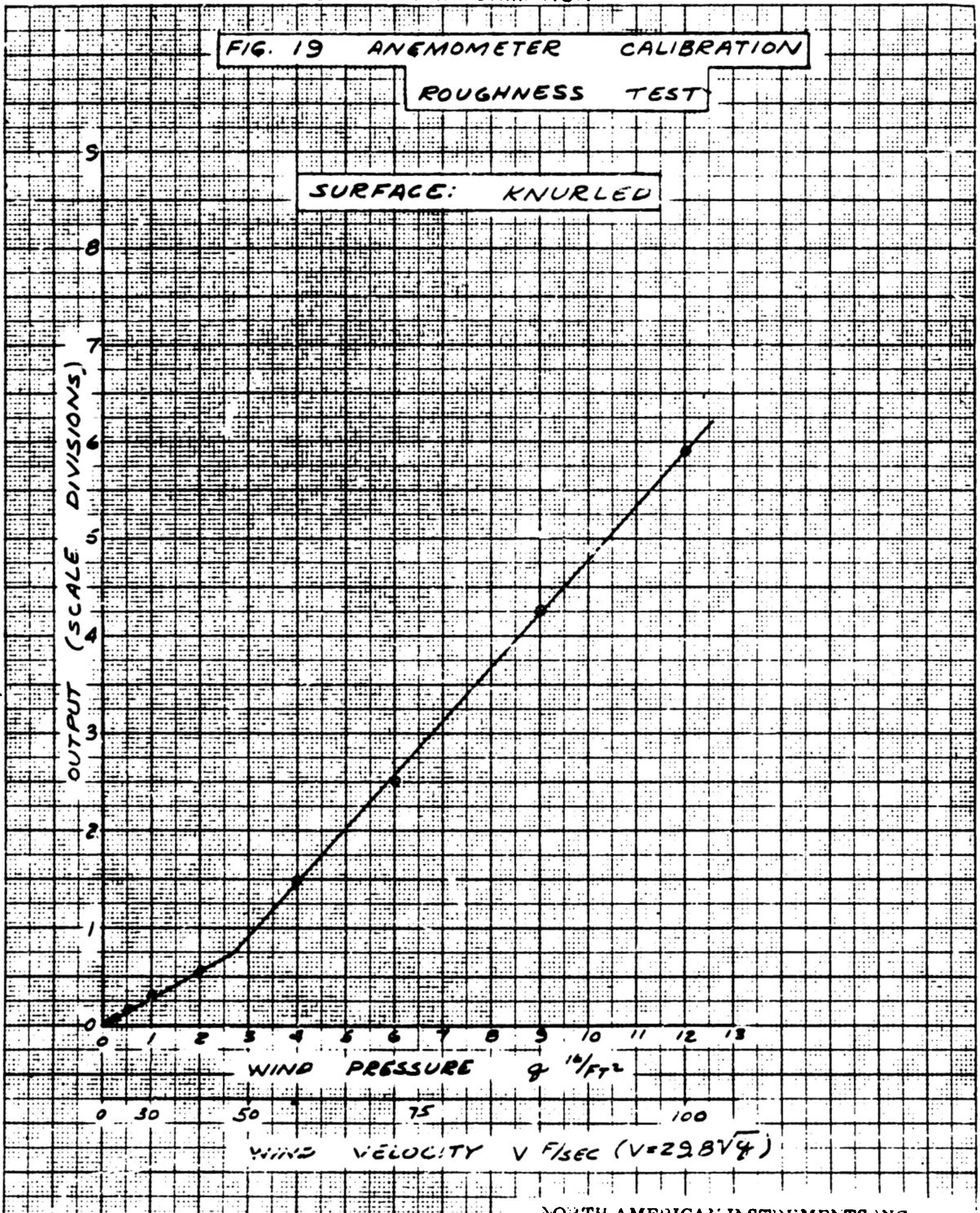

NORTH AMERICAN INSTRUMENTS INC.

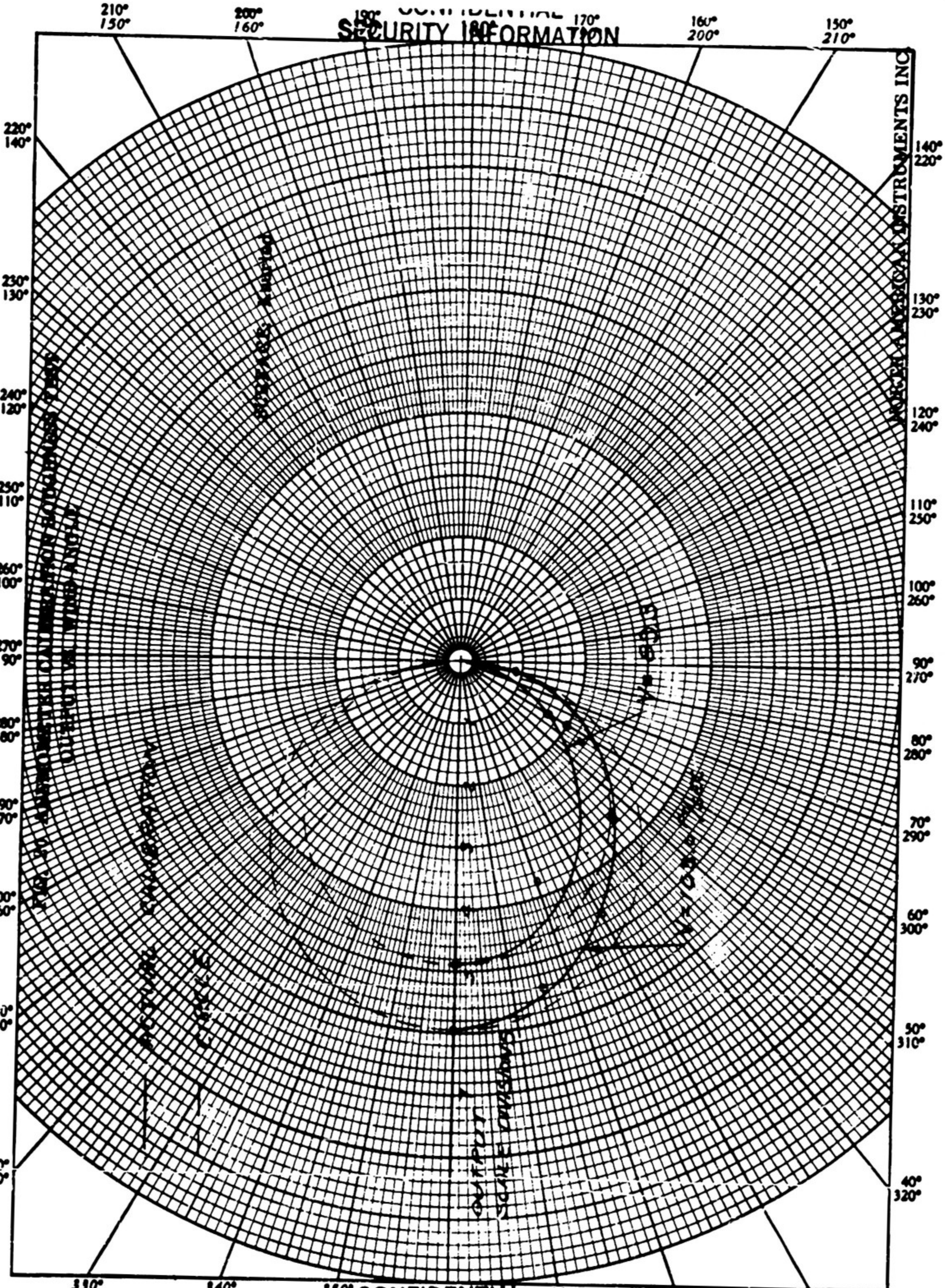

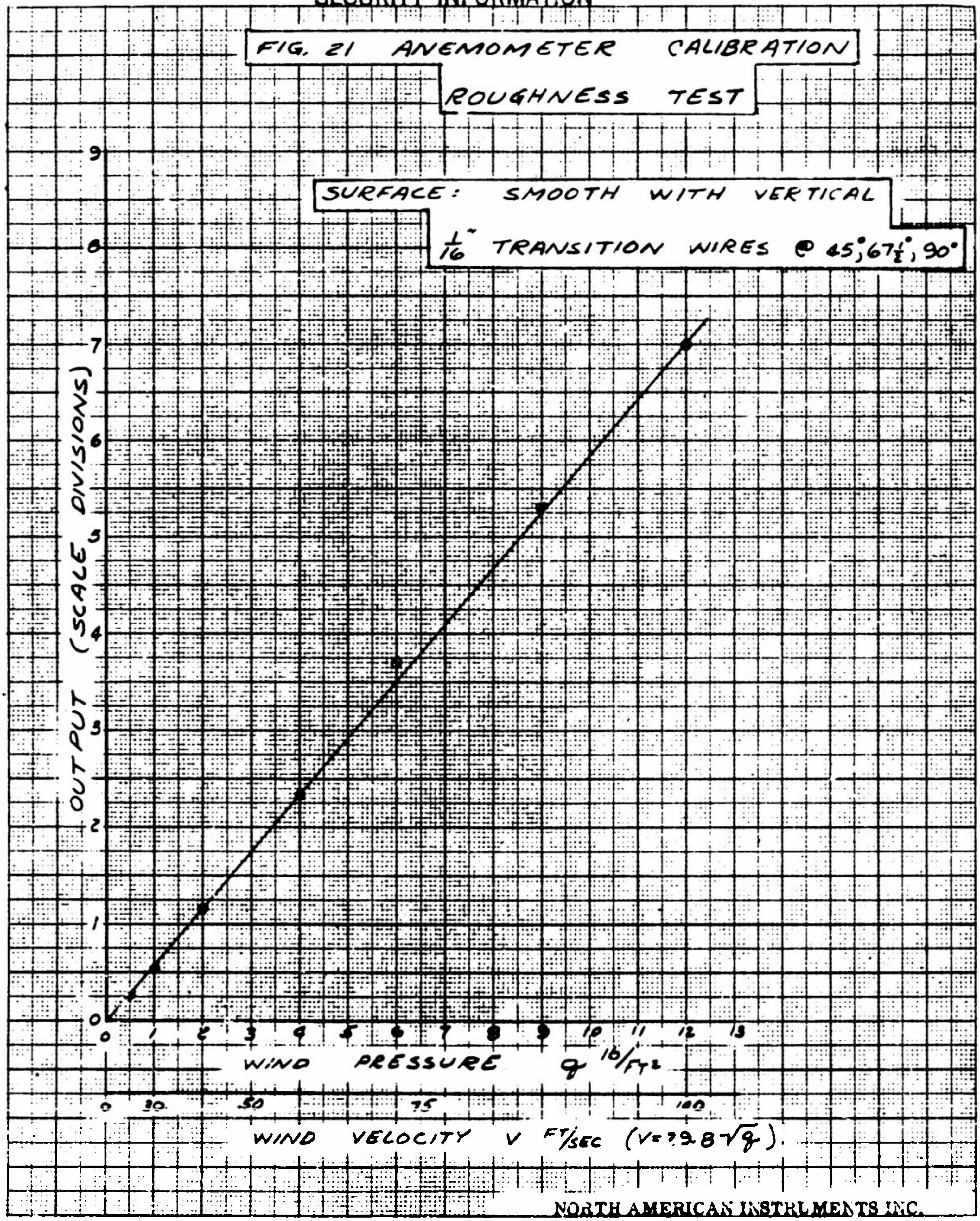

FIG. 21 ANEMOMETER CALIBRATION
ROUGHNESS TEST

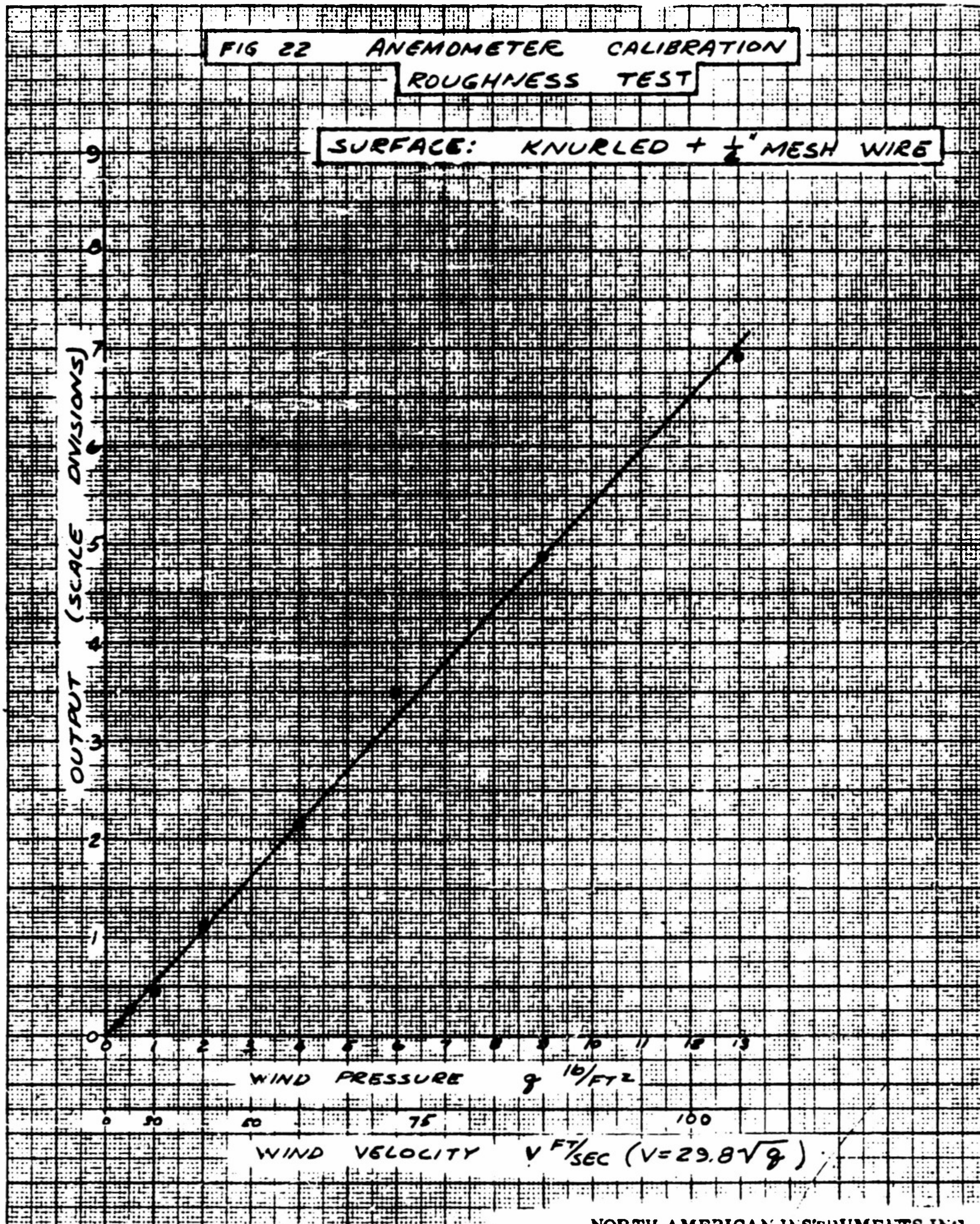
FIG 22 ANEMOMETER CALIBRATION
ROUGHNESS TEST
SURFACE: KNURLED + ¼" MESH WIRE
OUTPUT (SCALE DIVISIONS)
0
1
2
3
4
5
6
7
8
9
0 1 2 3 4 5 6 7 8 9 10 11 12 13
WIND PRESSURE q lb/FT²
0 30 50 75 100
WIND VELOCITY V FT/SEC (V=29.8√q)
NORTH AMERICAN INSTRUMENTS INC.

is within 2 mph. The fluctuating lift characteristic was reduced with the maximum effect 5% of the drag at 60 mph.

The performance of the 1/4 inch mesh wire was considered adequate and the next step was aimed at the design of a surface configuration that would offer the same degree of roughness while being suitable from the point of view of manufacture and reproducibility. Vertical slots milled at uniform intervals around the cylinder proved to be the most practical design.

The first slotting tests were made using phenolic sleeves with slots 1/16" wide by 1/16" deep by 1/16" spacing. The wind pressure vs. output plot, Fig. 23 is linear, the largest deviation corresponding to 2 mph. The polar calibration, Fig. 24, is circular. The fluctuating lift effect was negligible up to 70 mph with the exception of a sharp peak at 15 mph where the lift was 14% of the drag.

To reduce the fluctuating lift peak a second arrangement with slots 1/8 inch wide, 1/16 inch deep and 1/8 inch spacing was tried. This configuration met all requirements. The calibration plot, Fig. 24, is linear within 1 mph up to 70 mph. The fluctuating lift no longer showed a peak and in no case exceeded 5% of the drag with an oscillation period in the order of 1/2 to 1 second. The corresponding error would be less than 2% in velocity and less than 5° in direction. The polar plot is shown in Fig. 25 and indicates cosine law response.

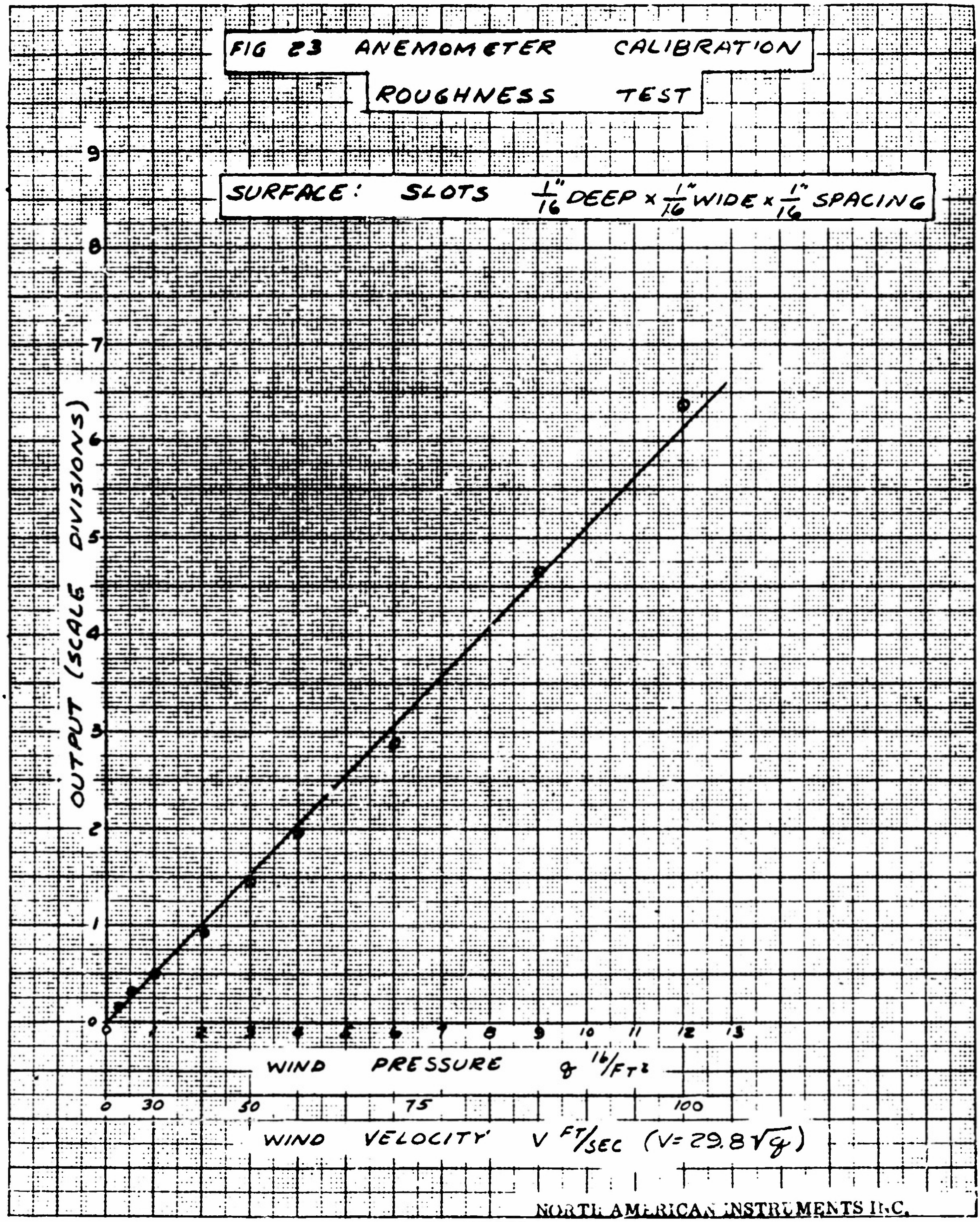
FIG 23 ANEMOMETER CALIBRATION
ROUGHNESS TEST
SURFACE: SLOTS 1/16" DEEP × 1/16" WIDE × 1/16" SPACING
OUTPUT (SCALE DIVISIONS)
0
1
2
3
4
5
6
7
8
9
0 1 2 3 4 5 6 7 8 9 10 11 12 13
WIND PRESSURE q lb/FT²
0 30 50 75 100
WIND VELOCITY V FT/SEC (V=29.8√q)
NORTH AMERICAN INSTRUMENTS INC.

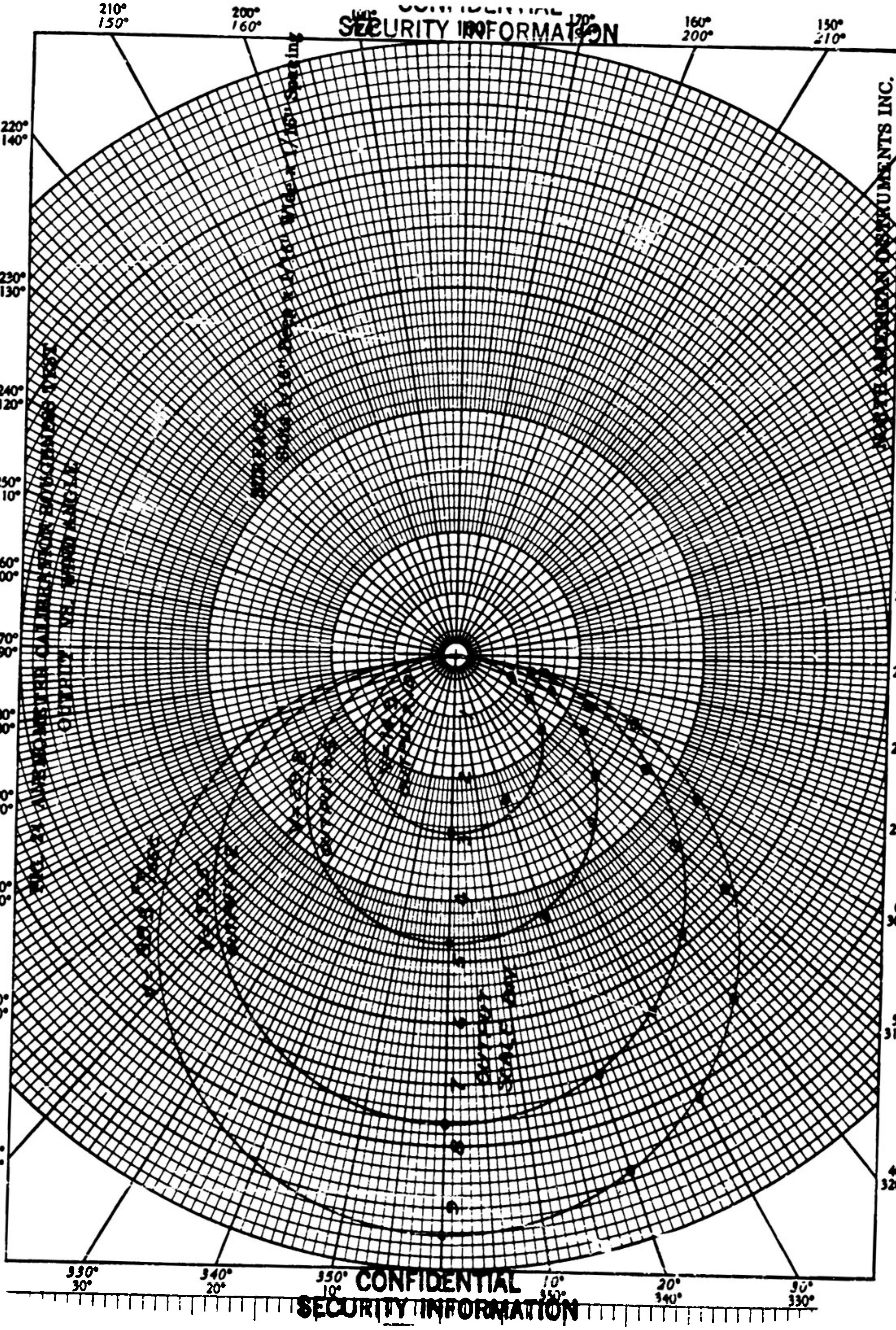

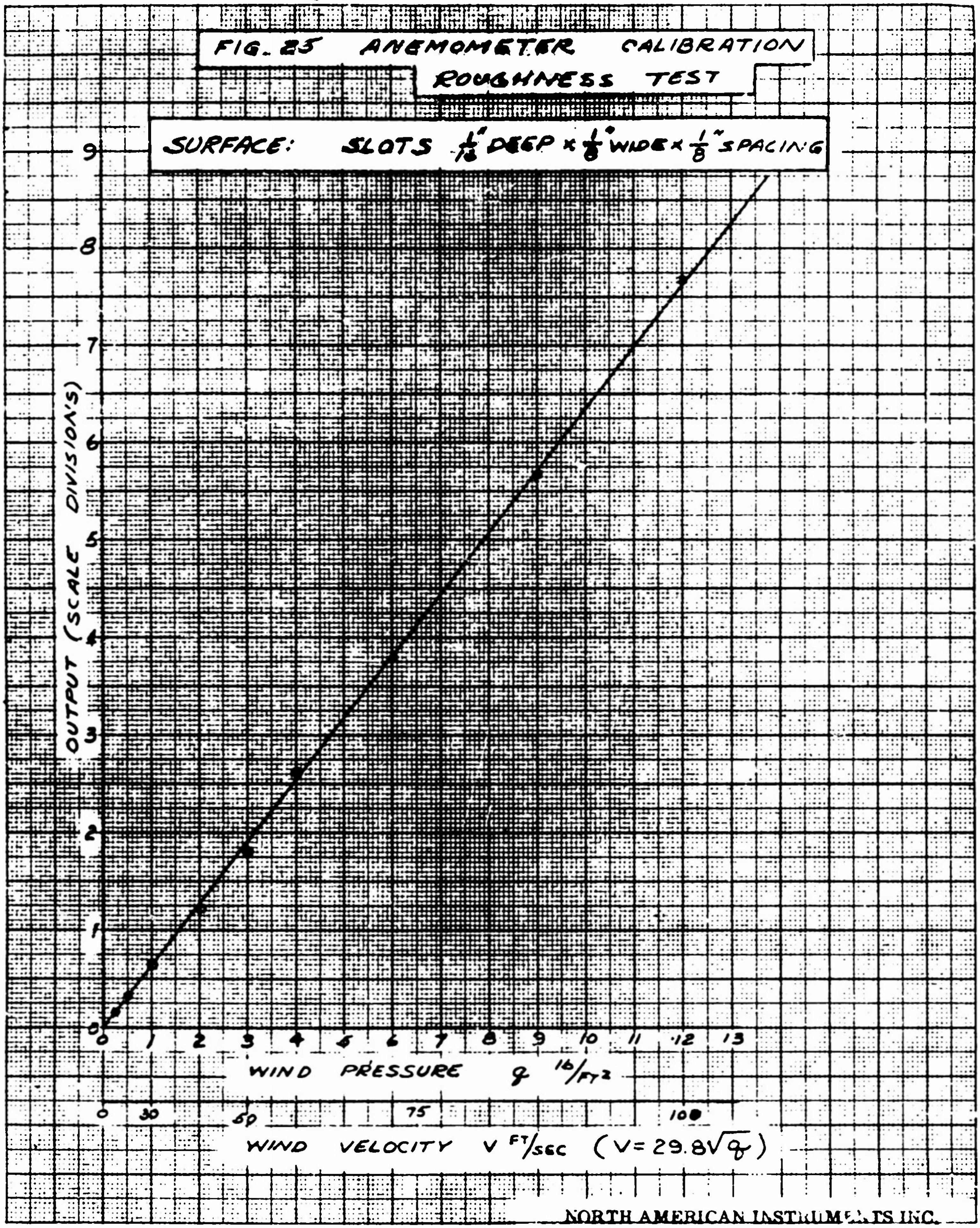
FIG. 25 ANEMOMETER CALIBRATION
ROUGHNESS TEST
SURFACE: SLOTS 1/16" DEEP × 1/8" WIDE × 1/8" SPACING
OUTPUT (SCALE DIVISIONS)
0
1
2
3
4
5
6
7
8
9
0 1 2 3 4 5 6 7 8 9 10 11 12 13
WIND PRESSURE q lb/FT²
0 30 50 75 100
WIND VELOCITY V FT/SEC (V = 29.8√q)
NORTH AMERICAN INSTRUMENTS INC.

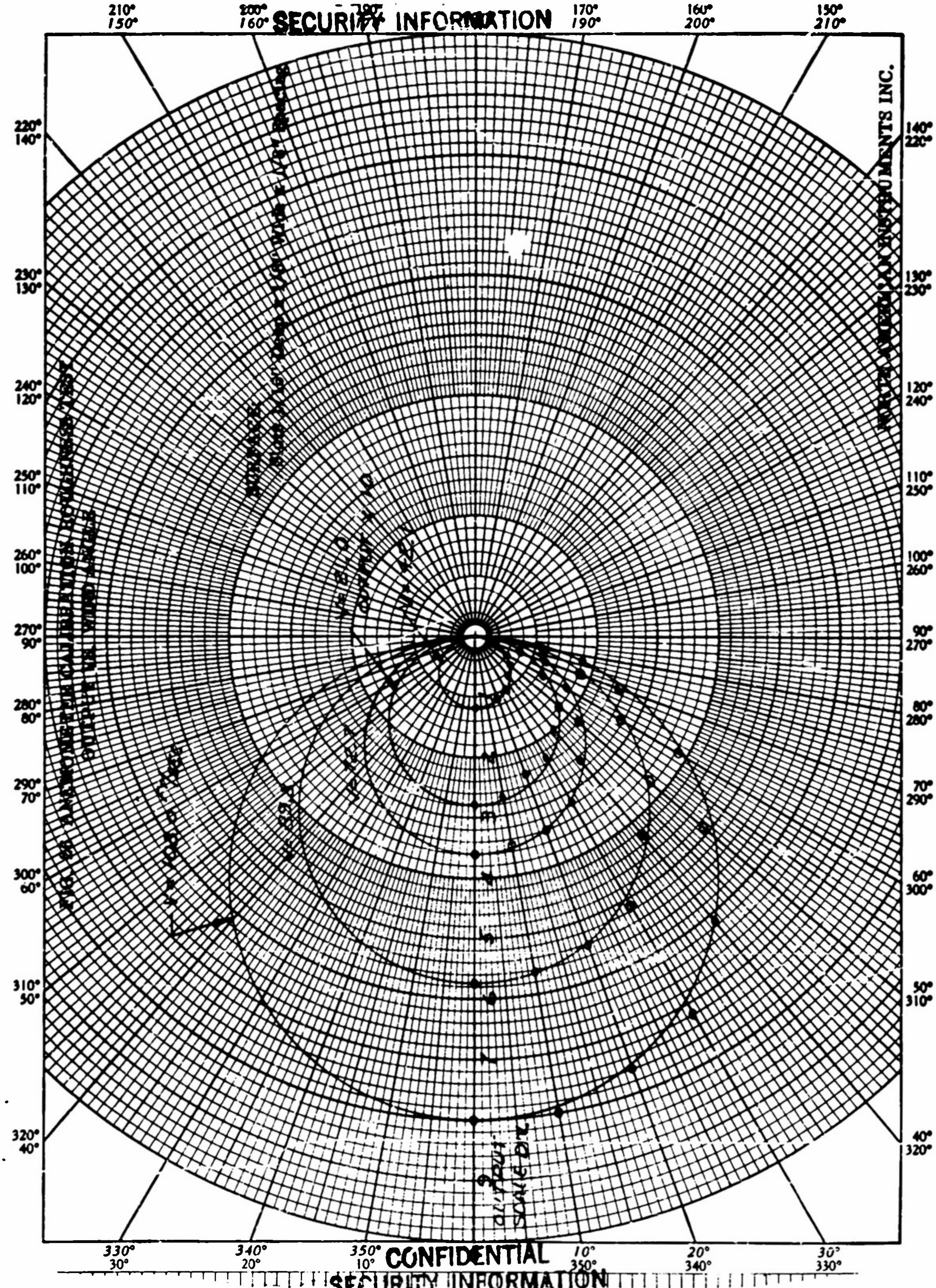

On the basis of the test results, the 1/8 inch slot arrangement was chosen as the configuration to be used in the second prototype now being built, and represents the best compromise in regard to linearity, component resolution, and stability.

REFERENCES

1. Sherlock, R. H. and Stout, M. B., Wind Structure in Winter Storms, Journal of the Aeronautical Sciences, Vol. 5, 1937.

2. Helfand, B., Preliminary Wind Studies for LOKI; Quarterly Report North American Instruments, Inc., Pasadena, California, Oct to Dec 1952.

3. MacCready, P. B. Jr., Investigation of Atmospheric Turbulence, Ph D. Thesis, California Institute of Technology, Pasadena, California, 1952.

4. Anderson, L. J., Captive Balloon Equipment for Low-Level Meteorological Soundings; Bulletin of the American Meteorological Society, Vol. 28, No. 8, Oct 1947.

5. King, L. V., On the Convection of Heat from Small Cylinders in a Stream of Fluid: Determination of the Convection Constants of Small Platinum Wires with Applications to Hot Wire Anemometry; Phil. Trans. Roy. Soc. (London) Ser. A, Vol. 214, 1914.

6. Corrsin, S., Extended Applications of the Hot Wire Anemometer; NACA TN No. 1864, California Institute of Technology, April 1949.

7. Bollay, E., and Helfand, B., Design and Development of a Wind Correction Computer for Use with M33 Director in the Fire Control for LOKI Rockets; Quart. Rpt. North American Instruments Inc. Pasadena, Calif, Jul 1, 1952

8. Goldstein, S., Editor, Modern Developments in Fluid Dynamics Vol II, Oxford University Press.

UNCLASSIFIED

AD 140888

CLASSIFICATION CHANGED
TO: UNCLASSIFIED
FROM CONFIDENTIAL
AUTHORITY:

USAMC ltr, 26 MAR 81

UNCLASSIFIED